AD-A143 592 FINITE TEMPERATURE EFFECTS ON THE EVOLUTION OF IONOSPHERIC BARIUM CLOUDS I..(U) NAVAL RESEARCH LAB WASHINGTON DC S T ZALESAK ET AL. 24 JUL 84 NRL-MR-5346 1/1

UNCLASSIFIED F/G 4/1 NL

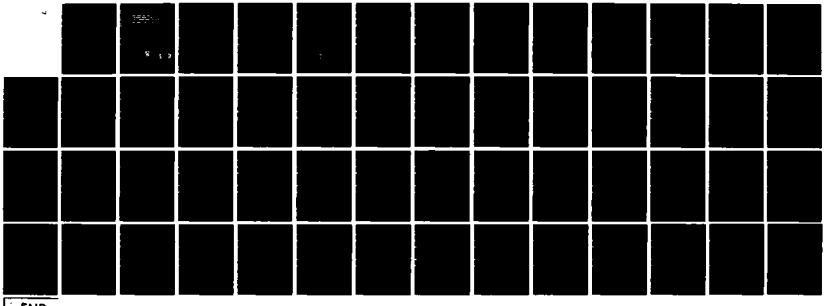

END

FILMED

DTIC

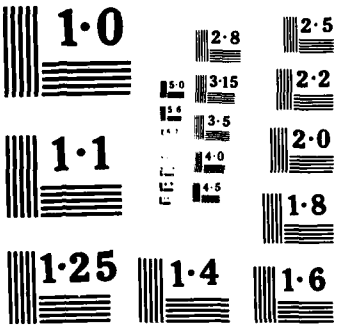
1·0
1·1
1·25
1·4
1·6
1·8
2·0
2·2
2·5
2·8
3·15
3·5
4·0
4·5

NRL Memorandum Report 5346

Finite Temperature Effects on the Evolution of Ionospheric Radium Clouds in the Presence of a Conducting Background Ionosphere

II. A Finite Altitude Incompressible Background Ionosphere

S. T. ZALESAK, P. K. CHATURVEDI,* S. L. OSSAKOW, AND I. A. FEDDER

Geophysical and Plasma Dynamics Branch
Plasma Physics Division

Science Applications, Inc.
McLean, VA 22102

July 26, 1984

This report was sponsored by the Defense Nuclear Agency under Subtask S99QMXBC, work unit 00157 and work unit title "Plasma Structure Evolution."

NAVAL RESEARCH LABORATORY
Washington, D.C.

AD-A143592

UNCLASSIFIED

REPORT DOCUMENTATION PAGE

1a REPORT SECURITY CLASSIFICATION UNCLASSIFIED	1b RESTRICTIVE MARKINGS
2a SECURITY CLASSIFICATION AUTHORITY	3 DISTRIBUTION AVAILABILITY OF REPORT Approved for public release; distribution unlimited.
2b DECLASSIFICATION/DOWNGRADING SCHEDULE	
4 PERFORMING ORGANIZATION REPORT NUMBER(S) NRL Memorandum Report 5346	5 MONITORING ORGANIZATION REPORT NUMBER(S)
6a NAME OF PERFORMING ORGANIZATION Naval Research Laboratory 6b OFFICE SYMBOL (If applicable) Code 4780	7a NAME OF MONITORING ORGANIZATION
6c ADDRESS (City, State and ZIP Code) Washington, DC 20375	7b ADDRESS (City, State and ZIP Code)
8a NAME OF FUNDING/SPONSORING ORGANIZATION Defense Nuclear Agency 8b OFFICE SYMBOL (If applicable)	9 PROCUREMENT INSTRUMENT IDENTIFICATION NUMBER
8c ADDRESS (City, State and ZIP Code) Washington, DC 20305	10 SOURCE OF FUNDING NOS PROGRAM ELEMENT NO: 62715H; PROJECT NO:; TASK NO:; WORK UNIT NO: DN580-072
11 TITLE (Include Security Classification) (See page ii)	

12 PERSONAL AUTHOR(S)
Zalesak, S.T., Chaturvedi, P.K.,* Ossakow, S.L., and Fedder, J.A.

13a TYPE OF REPORT	13b TIME COVERED	14 DATE OF REPORT (Yr., Mo., Day)	15 PAGE COUNT
Interim	FROM 10/83 TO 10/84	July 24, 1984	55

16 SUPPLEMENTARY NOTATION
*Science Applications Inc., McLean, VA 22102 (Continues)

17 COSATI CODES			18 SUBJECT TERMS (Continue on reverse if necessary and identify by block number)
FIELD	GROUP	SUB GR	Barium clouds; Ionospheric barium clouds; Striations; Plasma clouds; Bifurcation of barium clouds

19 ABSTRACT (Continue on reverse if necessary and identify by block number)

We show that under realistic ionospheric conditions, barium ion clouds hundreds of meters in diameter can be long-lived, quasi-stable, nonbifurcating structures. These structures may resemble "tadpoles," with a dense head, steep density gradients at the front, and a long, less dense tail. We assume that these structures are the final products of the recursive bifurcation of a considerably larger barium ion cloud, i.e., striations. The realistic ionospheric conditions to which we refer consist of a barium ion cloud with ion temperatures T_i of approximately 1000°K, coupled electrically to a background ionosphere of lower compressibility than itself, i.e., and F region. We show analytically that this combination of finite T_i and relatively incompressible background results in an effective diffusion of barium plasma, but more importantly, of total magnetic-field-line-integrated Pedersen conductivity, Σ_P. The diffusion coefficient has a special form which allows the inner portions of the cloud to diffuse slowly, giving the cloud a long lifetime,

(Continues)

20 DISTRIBUTION/AVAILABILITY OF ABSTRACT	21 ABSTRACT SECURITY CLASSIFICATION
UNCLASSIFIED/UNLIMITED X SAME AS RPT. DTIC USERS	UNCLASSIFIED

22a NAME OF RESPONSIBLE INDIVIDUAL	22b TELEPHONE NUMBER (Include Area Code)	22c OFFICE SYMBOL
S. T. Zaleask	(202) 767-3215	Code 4780

DD FORM 1473, 83 APR EDITION OF 1 JAN 73 IS OBSOLETE

UNCLASSIFIED

11. TITLE (Include Security Classification)

Finite Temperature Effects on the Evolution of Ionospheric Barium Clouds in the Presence of a Conducting Background Ionosphere
I. A High Altitude Incompressible Background Ionosphere

16. SUPPLEMENTARY NOTATION (Continued)

This research was sponsored by the Defense Nuclear Agency under Subtask S99QMXBC, work unit 00102 and work unit title "Plasma Structure Evolution."

19. ABSTRACT (Continued)

and allows the outer, less dense portions of the cloud to diffuse rapidly, preventing cloud bifurcation. Numerical simulations of the full nonlinear dynamics are then used to show that this diffusion does in fact give rise to quasi-stable barium striations hundreds of meters in diameter. These findings are consistent with the linear analysis of *Francis and Perkins* (1975).

CONTENTS

FINITE TEMPERATURE EFFECTS ON THE EVOLUTION OF IONOSPHERIC BARIUM CLOUDS IN THE PRESENCE OF A CONDUCTING BACKGROUND IONOSPHERE

I. A High Altitude Incompressible Background Ionosphere

1. Introduction

The nonlinear evolution of an artificial plasma cloud (e.g., a barium ion cloud) released in the earth's ionosphere is characterized by an overall bulk $\underline{E} \times \underline{B}$ motion, a one-sided steepening of plasma gradients, and by bifurcation [see Ossakow, 1979; Ossakow et al., 1982 and references therein] a process which we define here to mean the splitting of the cloud into two or more pieces. These pieces are sometimes referred to as "striations". All of the above motion and the resultant plasma structures are observed to be magnetic-field-aligned. That is, the plasma motion parallel to magnetic field lines consists primarily of diffusion and falling, while the perpendicular plasma motion is virtually identical for all plasma along a given field line. Hence one's best view of the structuring of the cloud is from a vantage point looking parallel to the magnetic field $\underline{B}$. This simplified description of barium cloud dynamics, seen along a line of sight parallel to $\underline{B}$, is depicted in Fig. 1. The sequence of drifting, steepening and bifurcating is, for sufficiently large striations, recursive: each striation becomes a new cloud which in turn forms its own striations. In the absence of some dissipative mechanism, it is believed that this process would continue indefinitely. In reality, the striation size becomes small enough to be comparable to the characteristic scale lengths of physical dissipation mechanisms, and further bifurcation ceases. A previous study by McDonald et al. [1981] attempted to quantify this concept within the context of a "one-level model", a mathematical model in which all conducting plasma was constrained to lie in a single two-dimensional plane perpendicular to the magnetic field. Implicit in

Manuscript approved March 15, 1984.

this model is the assignment of a single Pedersen mobility and hence compressibility to both the barium and background ionospheric plasma. In this model, the leading candidate for a dissipative mechanism is the ambipolar diffusion of electrons caused by electron-ion collisions. Using this mechanism, McDonald et al. [1981] calculated final unbifurcating striation sizes (from a so-called U shaped curve) for barium clouds of ~ 20 m (perpendicular to B). However, there is experimental evidence for the existence of long-lived "blobs" of plasma several hundred meters in diameter. The apparent stability of such large plasma structures has yet to find a satisfactory explanation within the one-level model. Ossakow et al. [1981] proposed including a zero temperature second level compressible background ionosphere below the cloud (see Scannapieco et al., 1976). This would allow image striations to build up and allow the conductivity in a striation to be amplified. This in turn would allow for larger conductivity ratios than if one had just a one level cloud. In turn, this could result in kilometer size unbifurcating striations by extrapolating the U shaped curve of McDonald et al. [1981] to higher conductivity ratios.

Here we postulate that the existence of a conducting background plasma with ion Pedersen mobility different from that of the barium plasma, combined with the finite temperature of the barium plasma, may allow the existence of stable striations with scale sizes of hundreds of meters. The essence of the mechanism is a phenomenon commonly referred to as "end shorting" first investigated in the context of barium clouds by Shiau and Simon [1974], who considered a completely incompressible background ionosphere, and showed that the normal electron ambipolar diffusion rates would be replaced by some fraction of the much higher ion diffusion rates caused by collisions of ions with neutrals. Francis and Perkins [1975] generalized the work of Shiau and Simon [1974] by

considering the cases of both incompressible and compressible background ionospheres. They concurred with Shiau and Simon [1974] that incompressible backgrounds exert a stabilizing influence, but noted that compressible backgrounds are destabilizing. In contrast, Vickrey and Kelley [1982] concluded that a background (compressible) E region should exert a stabilizing influence on high latitude irregularities. We shall address the question of the correctness of the above two analyses in a later paper. For the moment we note that: 1) Francis and Perkins [1975] performed a rigorous stability analysis of the problem; Vickrey and Kelley [1982] did not; 2) Francis and Perkins [1975] self-consistently included image formation (compressibility) in both the cloud and the background; Vickrey and Kelley [1982] did not (they took a passive load model); 3) Vickrey and Kelley [1982] included recombination chemistry; Francis and Perkins [1975] did not.

Our own conclusions are based on our view of barium cloud dynamics as consisting of a two-stage feed-back loop:

1) At any given time, the distribution of plasma density will, through the effect of these distributions on magnetic-field-line integrated Pedersen and Hall conductivities, bring about the creation of polarization electric fields whose purpose it is to maintain quasi-neutrality;

2) these electric fields, through Hall and Pedersen mobilities, affect the velocity of the plasma, which in turn affects the distribution of plasma density at the next instant of time.

We emphasize that it is only through its influence on magnetic-field-line integrated Pedersen and Hall conductivities that a change in plasma distribution [e.g., diffusion] will affect the polarization fields, which are the engine of plasma structure.

In the present study we have isolated the "enhanced" difusive effects (due to finite temperature effects and a two level model, where only ion-neutral collisions are included) on barium cloud striation evolution. A major conclusion derived from the nonlinear numerical simulation results presented here is that coupling to a nearly incompressible background ionosphere, i.e., an F region, can result in a cessation of striation bifurcation in F region ionospheric barium clouds.

In addition, a simplified analysis of the equation for the time evolution of the total field line integrated Pedersen conductivity shows that coupling to a compressible background ionosphere, i.e., E region, would result in destabilization of the striations (see Eq. (4-36) and the discussion following). Both of these results are consistent with the linear analysis of Francis and Perkins [1975].

In section 2 we describe the motion of ionospheric plasma and in section 3 the mathematical model is presented. Section 4 presents a simplified two level model. Section 5 describes the diffusion characteristics for a simplified two level model with a nearly incompressible background. Numerical simulation results using an incompressible background are presented in section 6. Section 7 presents the conclusions and thoughts on future work.

2. The Motion of Ionospheric Plasma

We shall be concerned here with the motion of plasma consisting of ions and electrons in the presence of a neutral gas and magnetic field $\underline{B}$, subject to an external force. We shall also be interested in the electric current $\underline{J}$ arising from the differential motion of the various species comprising the plasma. In the course of deriving the equations we make the following assumptions:

1) We assume the plasma can be adequately described by the fluid approximation. This assumes that the effective collision rate of each plasma species with itself is sufficiently high to maintain near Maxwellian distribution functions on time scales short compared to the times of interest, and is well satisfied for the plasmas we treat here.

2) We assume that the electric fields $\underline{E}$ are electrostatic (i.e., $\nabla \times \underline{E} = 0$) and hence can be described using a scalar potential ϕ such that $\underline{E} = -\nabla\phi$. Note that this implies $\partial\underline{B}/\partial t = 0$. The validity of this assumption can be related to the fact that the Alfven velocity is much larger than any other propagation speed of interest for the plasmas we treat here. The assumption is also checked a posteriori by verifying that the calculated currents and displacement currents produce negligible time variations in $\underline{B}$ which in turn produce negligible $\nabla \times \underline{E}$.

3) We assume plasma quasi-neutrality; that is,

$$\sum n_i q_i = n_e e \tag{2.1}$$

where n is the number density, q is ion species charge, e is the electron charge, the subscripts i and e refer to ions and electrons respectively, and the sum is taken over all ion species. This assumption is a statement

that the Debye length is small compared to all length scales of interest, and again can be verified a posteriori by evaluating $\nabla \cdot \underline{E}$. Note that this assumption implies that $\nabla \cdot \underline{J} = 0$, where $\underline{J}$ is the electric current.

In addition to the above there are some other assumptions which, while they are not essential to the basic model, are nonetheless valid for many of the physical situations which we shall treat and impart a simplicity which we shall find convenient here.

4) We assume the electrostatic potential ϕ to be constant along magnetic field lines. As we shall see later, the electrical conductivity along magnetic field lines is much greater than that perpendicular to magnetic field lines, meaning that appreciable differences in potential along a field line will quickly be reduced by the resultant current. This assumption will break down for sufficiently small scale lengths perpendicular to the magnetic field, and for sufficiently large distances along the magnetic field.

5) We assume that the inertial terms in the plasma species momentum equations, i.e., the left hand side of Equation (2.3), are negligible with respect to the other terms in the equation. This assumption is justified whenever the time scales of interest are longer than the mean time between collisions for ions.

6) We neglect collisions between ions and electrons and between ions of different species. Later we shall also neglect collisions of electrons with neutrals. There are two reasons for this. First, the ion-neutral collision term ν_{in} can be shown to be the dominant term in the diffusion physics we consider here. (One must be careful, however, since these same assumptions will yield <u>zero</u> diffusion when the background conductivity is set to zero. To obtain the correct electron ambipolar rate in this limit,

the electron-ion and electron-neutral collision terms must be retained. We are not interested in this limit in this paper). Second, although exact closed form expressions for the ion and electron velocities in terms of the applied forces is possible when ion-electron collisions are retained [Fedder, 1980], the expressions are considerably more complex than those given below.

The continuity and momentum equations describing a single ion species and its associated electrons are:

$$\frac{\partial n_\alpha}{\partial t} + \nabla \cdot (n \underline{v}_\alpha) = 0 \tag{2.2}$$

$$(\frac{\partial}{\partial t} + \underline{v}_\alpha \cdot \nabla)\underline{v}_\alpha = \frac{q_\alpha}{m_\alpha} (\underline{E} + \frac{\underline{v}_\alpha \times \underline{B}}{c}) - \nu_{\alpha n}(\underline{v}_\alpha - \underline{U}_n)$$

$$- \frac{\nabla P_\alpha}{n_\alpha m_\alpha} + \underline{g} \tag{2.3}$$

where the subscript α takes on values i and e (denoting ions and electrons, respectively), n is the number density, $\underline{v}$ is the fluid velocity, P is pressure, $\underline{E}$ is the electric field, $\underline{g}$ is the gravitational acceleration, q is the charge, $\nu_{\alpha n}$ is the collision frequency with the neutral gas, $\underline{U}_n$ is the neutral wind velocity, c is the speed of light, and m is the particle mass. We can rewrite this equation as

$$\underline{F}_\alpha/m_\alpha + \frac{q_\alpha}{m_\alpha c} (\underline{v}_\alpha \times \underline{B}) - \nu_{\alpha n} \underline{v}_\alpha = 0 \tag{2.4}$$

where

$$\underline{F}_\alpha \equiv q_\alpha \underline{E} + m_\alpha g + \nu_{\alpha n} m_\alpha \underline{U}_\alpha - \nabla p_\alpha / n_\alpha$$

$$- \left(\frac{\partial}{\partial t} + \underline{v}_\alpha \cdot \nabla\right) \underline{v}_\alpha m_\alpha \qquad (2.5)$$

If we place ourselves in a Cartesian coordinate system in which $\underline{B}$ is aligned along the z axis, and if we treat $\underline{F}_\alpha$ as a given quantity then a componentwise evaluation of Equation (2.4) yields a set of three equations in three unknowns, the three components of $\underline{v}_\alpha$. The formal solution is

$$\underline{v}_{\alpha\perp} = k_{1\alpha} \underline{F}_{\alpha\perp} + k_{2\alpha} \underline{F}_{\alpha\perp} \times \hat{\underline{z}} \qquad (2.6)$$

$$\underline{v}_{\alpha\parallel} = k_{o\alpha} \underline{F}_\parallel \qquad (2.7)$$

where

$$k_{1\alpha} = \frac{\nu_{\alpha n}}{\Omega_\alpha} \frac{c}{|q_\alpha B|} \left[1 - \frac{(\nu_{\alpha n}/\Omega_\alpha)^2}{1 + (\nu_{\alpha n}/\Omega_\alpha)^2}\right] \qquad (2.8)$$

$$k_{2\alpha} = \frac{c}{q_\alpha B} \left[1 - \frac{(\nu_{\alpha n}/\Omega_\alpha)^2}{1 + (\nu_{\alpha n}/\Omega_\alpha)^2}\right] \qquad (2.9)$$

$$k_{o\alpha} = (m_\alpha \nu_{\alpha n})^{-1} \qquad (2.10)$$

$$\hat{\underline{z}} \equiv \underline{B}/|B| \qquad (2.11)$$

$$\Omega_\alpha \equiv \left|\frac{q_\alpha B}{m_\alpha c}\right| \qquad (2.12)$$

The vector subscripts $\perp$ and $\parallel$ refer to the components of the vector which are perpendicular and parallel respectively to $\hat{\underline{z}}$. The quantities k_1, k_2,

and k_o above are referred to as the Pedersen, Hall, and direct mobilities respectively. It should be pointed out that Equations (2.6) and (2.7) are only truly closed form expressions when the inertial terms (the last term on the right hand side of Equation (2.5)) are neglected, an assumption we have made previously. Typical ranges for collision frequencies are: $\nu_{in} \sim 30$ sec^{-1}, $\nu_{en} \sim 800$ sec^{-1} at 150 km altitude; and $\nu_{in} \sim 10^{-1}$ sec^{-1}, $\nu_{en} \sim 1$ sec^{-1} at 500 km altitude.

As we will see later, we will use the concept of "layers" to distinguish the various ion species, so for the moment we consider only a single ion species, denoted by subscript i, and the associated electrons, denoted by subscript e. We also consider only singly charged ions so that $q_i = e$ and $q_e = -e$. Noting that $\nu_{en}/\Omega_e \approx 0$, we obtain

$$k_{1i} = \frac{\nu_{in}}{\Omega_i} R_i \frac{c}{e|B|} \tag{2.13}$$

$$k_{1e} = 0 \tag{2.14}$$

$$k_{2i} = R_i \frac{c}{eB} \tag{2.15}$$

$$k_{2e} = -\frac{c}{eB} \tag{2.16}$$

where

$$R_i \equiv (1 + \nu_{in}^2/\Omega_i^2)^{-1} \tag{2.17}$$

We now define the perpendicular current

$$\underline{J}_\perp \equiv \sum_\alpha n_\alpha q_\alpha \underline{v}_{\alpha\perp} \tag{2.18}$$

Substituting Equations (2.13) through (2.15) and (2.6) into Equation (2.18), and using the quasi-neutrality approximation

$$n_i \approx n_e \equiv n \tag{2.19}$$

we obtain

$$\underline{J}_\perp = \frac{\nu_{in}}{\Omega_i} R_i \frac{nc}{|B|} \underline{F}_{i\perp} + \frac{nc}{B} (R_i \underline{F}_{i\perp} + \underline{F}_{e\perp}) \times \hat{\underline{z}} \tag{2.20}$$

For the barium cloud problem we shall treat here, we shall only consider neutral winds, electric fields, gravity, and pressure gradients as external forces. Hence

$$\underline{F}_{i\perp} = e \underline{E}_\perp + m_i \underline{g}_\perp + \nu_{in} m_i \underline{U}_{n\perp} - \nabla P_i/n \tag{2.21}$$

$$\underline{F}_{e\perp} = - e \underline{E}_\perp + m_e \underline{g}_\perp - \nabla P_e/n \tag{2.22}$$

Note that we have neglected the small term $\nu_{en} m_e \underline{U}_{n\perp}$ in Equation (2.22). We obtain

$$\underline{J}_\perp = \frac{\nu_{in}}{\Omega_i} R_i \frac{nc}{|B|} (e \underline{E}_\perp + m_i \underline{g}_\perp + \nu_{in} m_i \underline{U}_{n\perp} - \nabla P_i/n)$$

$$+ R_i \frac{nc}{B} \left[e\underline{E}_\perp (1 - R_i^{-1}) + (m_i + \frac{m_e}{R_i}) \underline{g}_\perp + \nu_{in} m_i \underline{U}_{n\perp} \right.$$

$$\left. - \nabla P_i/n - \nabla P_e R_i^{-1}/n \right] \times \hat{z} \qquad (2.23)$$

Since $0.01 < R_i < 1.0$ we may neglect m_e/R_i with respect to m_i. Defining the Pedersen conductivity

$$\sigma_p \equiv R_i \frac{\nu_{in}}{\Omega_i} \frac{nce}{|B|} \qquad (2.24)$$

and noting that $1 - R_i^{-1} = - \nu_{in}^2/\Omega_i^2$ we obtain

$$\underline{J}_\perp = \sigma_p \left[\underline{E}_\perp + \frac{m_i}{e} \underline{g}_\perp + \nu_{in} \frac{m_i}{e} \underline{U}_{n\perp} - \frac{\nabla P_i}{ne} \right.$$

$$+ \frac{B}{|B|} \left(- \frac{\nu_{in}}{\Omega_i} \underline{E}_\perp + \frac{\Omega_i m_i}{\nu_{in} e} \underline{g}_\perp + \Omega_i \frac{m_i}{e} \underline{U}_{n\perp} \right.$$

$$\left. \left. - \frac{\Omega_i}{\nu_{in} ne} (\nabla P_i + R_i^{-1} \nabla P_e) \right) \times \hat{z} \right] \qquad (2.25)$$

Our need for an expression for $\underline{J}_\perp$ stems from our need for its divergence to evaluate $\nabla \cdot \underline{J}$ (= 0 by quasi-neutrality), as we shall see in the next section.

3. Mathematical Model

We shall model our physical system using a simplified model as depicted in Figure 2. The magnetic field lines are assumed to be straight, to be aligned along the z axis of our cartesian coordinate system, and to terminate in insulators at $z = \pm \infty$. The plasma of interest is threaded by these magnetic field lines, and is divided into thin planes or "layers" of plasma perpendicular to the magnetic field. Since we have neglected collisions between different plasma species, we may use the device of layers to treat multiple ion species at a single point in space simply by allowing multiple layers to occupy the same plane in space, one for each ion species. In this way a "layer" consists only of a single ion species and its associated electrons.

Our quasi-neutrality assumption demands that

$$\nabla \cdot \underline{J} = \frac{\partial}{\partial x} J_x + \frac{\partial}{\partial y} J_y + \frac{\partial}{\partial z} J_z = 0 \tag{3.1}$$

Integrating Equation (3.1) along z and noting from Figure 2 that J_z vanishes at $z = \pm \infty$ we obtain

$$\int_{\infty}^{+\infty} \nabla_\perp \cdot \underline{J}_\perp \, dz = 0 \tag{3.2}$$

where

$$\nabla_\perp \equiv \hat{\underline{x}} \frac{\partial}{\partial x} + \hat{\underline{y}} \frac{\partial}{\partial y} \tag{3.3}$$

From our model as depicted in Figure 2 we may approximate the integral in Equation (3.2) by a discrete sum

$$\sum_{k=1}^{K} \nabla_{\perp} \cdot \underline{J}_{\perp k} \Delta z_k = 0 \tag{3.4}$$

where the subscript k refers to the layer number, K is the total number of layers in the system, and Δz_k is the thickness of layer k measured along the magnetic field line. Within a layer, both the ion density n and the ion-neutral collision frequency ν_{in} are assumed to be constant along a magnetic field line. This enables us to introduce the three magnetic-field-line integrated quantities:

$$N_k \equiv n_k \Delta z_k \tag{3.5}$$

$$\Sigma_{pk} \equiv \sigma_{pk} \Delta z_k = N_k \left(\frac{\nu_{in}}{\Omega_i} R_1\right)_k \frac{ce}{|B|} \tag{3.6}$$

$$\Sigma_{hk} \equiv \left(\frac{\nu_{in}}{\Omega_i}\right)_k \Sigma_{pk} \tag{3.7}$$

By our assumption of equipotential magnetic field lines and electrostatic electric fields

$$\underline{E}_{\perp k}(x,y) = \underline{E}_o - \nabla_{\perp}\phi(x,y) \text{ for all } k \tag{3.8}$$

where $\underline{E}_o \equiv E_{ox}\hat{\underline{x}} + E_{oy}\hat{\underline{y}}$ is a constant, externally imposed electric field. Then Equation (3.4) becomes

$$\nabla_\perp \cdot \left[\sum_{k=1}^{K} (\Sigma_{pk}) \nabla_\perp \phi \right] + \sum_{k=1}^{K} H_k = \sum_{k=1}^{K} \nabla_\perp \cdot \underline{J}_{\perp k}^{ext} \tag{3.9}$$

where

$$H_k \equiv - \frac{\partial}{\partial x} \left(\Sigma_{hk} \frac{\partial \phi}{\partial y} \right) + \frac{\partial}{\partial y} \left(\Sigma_{hk} \frac{\partial \phi}{\partial x} \right)$$

$$= - \frac{\partial \phi}{\partial y} \frac{\partial \Sigma_{hk}}{\partial x} + \frac{\partial \phi}{\partial x} \frac{\partial \Sigma_{hk}}{\partial y} \tag{3.10}$$

$$\underline{J}_{\perp k}^{ext} \equiv \Sigma_{pk} \left[\frac{m_i}{e} \underline{g}_\perp + \nu_{in} \frac{m_i}{e} \underline{U}_{n\perp} - \frac{\nabla P_i}{ne} + \underline{E}_o \right.$$

$$+ \frac{B}{|B|} \left(\frac{\Omega_i m_i}{\nu_{in} e} \underline{g}_\perp + \Omega_i \frac{m_i}{e} \underline{U}_\perp - \frac{\Omega_i}{ne \nu_{in}} \left(\nabla P_i + R_i^{-1} \nabla P_e \right) \right.$$

$$\left. \left. - \frac{\nu_{in}}{\Omega_i} \underline{E}_o \right) \times \hat{\underline{z}} \right]_k \tag{3.11}$$

and the subscript k denoting layer number on terms within parenthesis operates on all terms within those parentheses.

The system of equations we must solve consists of (3.9)-(3.11) and an equation of continuity for each layer:

$$\frac{\partial N_k}{\partial t} + \nabla \cdot \left(N_k \underline{v}_{ik} \right) = 0 \qquad k=1, \ldots, K \tag{3.12}$$

where $\underline{v}_i$ is given by Eq. (2.6)-(2.12).

4. Simplified Two-Level Model

We make the following further simplifications in our model:

a) We find that for ionospheric barium clouds the currents parallel to $\underline{B}$ are carried primarily by electrons, and the motion of ions parallel to $\underline{B}$ consists primarily of a slow diffusion plus a bulk falling of the cloud to lower altitudes (since $\underline{g} \cdot \underline{B} \neq 0$). It is therefore sufficient to represent the ions as an array of two-dimensional planes or layers of plasma perpendicular to $\underline{B}$, each moving with the bulk "falling" velocity along $\underline{B}$, and hence to treat numerically only the transport of ions perpendicular to $\underline{B}$ within each layer.

b) We limit our discussion to a model consisting of only two layers or species of ions.

c) We assume that the ion neutral collision frequency ν_{in} is constant within a layer.

d) We assume that the only forces acting on the plasma are an external electric field $\underline{E}_o$ and pressure gradients.

With the above assumptions we have

$$\underline{J}_{\perp k}^{ext} = \Sigma_{pk}\left[\left(\underline{E}_o - \frac{\nabla P_i}{ne}\right)_k + \frac{B}{|B|}\left[-\frac{\nu_{in}\underline{E}_o}{\Omega_i} - \frac{\Omega_i}{ne\,\nu_{in}}\left(\nabla P_i + R_i^{-1}\nabla P_e\right)\right]_k \times \hat{\underline{z}}\right] \qquad (4.1)$$

If we assume $\underline{B}$ is along the positive z axis then $B/|B| = 1$ and we get

$$\nabla_\perp \cdot \underline{J}_{\perp k}^{ext} = \nabla_\perp \cdot \left(\Sigma_{pk}\left(\underline{E}_o - \frac{\nabla P_i}{ne}\right)_k\right) - \nabla_\perp \cdot \left(\Sigma_p \frac{\nu_{in}}{\Omega_i}\underline{E}_o \times \hat{\underline{z}}\right)_k + H_{pk} \qquad (4.2)$$

where

$$H_{pk} = - \nabla_\perp \cdot \left(\Sigma_p \frac{\Omega_i}{ne\, \nu_{in}} \left(\nabla P_i + R_i^{-1} \nabla P_e \right) \times \hat{z} \right)_k \tag{4.3}$$

Now

$$\left[\Sigma_p \frac{\Omega_i}{ne\, \nu_{in}} \right]_k = \left[R_i \frac{\nu_{in}}{\Omega_i} \frac{n\, c\, e}{|B|} \Delta z \frac{\Omega_i}{\nu_i ne} \right]_k$$

$$= \left[R_i \frac{c}{|B|} \Delta z \right]_k \tag{4.4}$$

which is a constant within a layer if ν_{in} is constant within a layer (one of our assumptions). Then

$$H_{pk} = - \nabla_\perp \cdot \left(\text{constant } \nabla \left(P_i + R_i^{-1} P_e \right) \times \hat{z} \right) = 0 \tag{4.5}$$

(since $\nabla_\perp \cdot (\nabla C \times \hat{z}) = 0$ for any scalar field C).

Our final equations to be solved are then

$$\frac{\partial N_k}{\partial t} + \nabla_\perp \cdot \left(N_k \underline{v}_{k\perp} \right) = 0 \qquad k=1,2 \tag{4.6}$$

$$\nabla_\perp \cdot \left[\left(\Sigma_{p1} + \Sigma_{p2} \right) \nabla_\perp \phi \right] + H = \underline{E}_o \cdot \nabla_\perp \left(\Sigma_{p1} + \Sigma_{p2} \right)$$

$$- \nabla_\perp \cdot \left(\Sigma_{p1} \frac{\nabla P_{i1}}{n_1 e} + \Sigma_{p2} \frac{\nabla P_{i2}}{n_2 e} \right) \tag{4.7}$$

where

$$H \equiv -\frac{\partial}{\partial x}\left[(\Sigma_{h1} + \Sigma_{h2})(\frac{\partial \phi}{\partial y} - E_{oy})\right] + \frac{\partial}{\partial y}\left[(\Sigma_{h1} + \Sigma_{h2})(\frac{\partial \phi}{\partial x} - E_{ox})\right] \tag{4.8}$$

Looking at Eq. (4.7) we notice that ϕ may be separated into two parts:

$$\phi = \phi_E + \phi_P \tag{4.9}$$

$$\nabla_\perp \cdot \left[(\Sigma_{p1} + \Sigma_{p2})\nabla_\perp \phi_E\right] + H = \underline{E}_o \cdot \nabla_\perp(\Sigma_{p1} + \Sigma_{p2}) \tag{4.10}$$

$$\nabla_\perp \cdot \left[(\Sigma_{p1} + \Sigma_{p2})\nabla_\perp \phi_P\right] = -\nabla_\perp(\Sigma_{p1}\frac{\nabla P_{i1}}{n_1 e} + \Sigma_{p2}\frac{\nabla P_{i2}}{n_2 e}) \tag{4.11}$$

For reasons which shall become clear as we progress, we shall regard ϕ_E as that part of the potential field which tends to drive the cloud toward bifurcation. In fact, Eq. (4.10) coupled with (4.6) just form the basic inviscid two-level equations [Scannapieco et al., 1976]. We shall regard ϕ_P as that part of the potential field which tends to diffuse or anti-diffuse the edges of the cloud. First let us look at solutions to (4.11). If ∇P_{i1} and ∇P_{i2} vanish at our boundaries, the unique solution consistent with zero Neumann boundary conditions (vanishing of the normal derivative of ϕ_P at the boundary) gives:

$$-(\Sigma_{p1} + \Sigma_{p2})\nabla_\perp \phi_P = \Sigma_{p1}\frac{\nabla P_{i1}}{n_1 e} + \Sigma_{p2}\frac{\nabla P_{i2}}{n_2 e} \tag{4.12}$$

In general, the motion resulting from the forces proportional to $\nabla\phi_P$, ∇P_{i1} and ∇P_{i2} will be quite complex, not describable as the simple

superposition of a shear and a diffusion. However, in the special case of one of the layers being uniform, e.g., N_2 and T_{i2} (T_i = ion temperature) hence Σ_{p2} and P_{i2} uniform, then

$$\nabla\phi_P = \frac{-\Sigma_{p1}}{\Sigma_{p1} + \Sigma_{p2}} \frac{\nabla P_{i1}}{n_1 e} \tag{4.13}$$

We shall now treat this special case. One may conveniently think of level 1 as representing the barium cloud and level 2 the uniform background ionosphere.

We now use the equation of state

$$P_i = n\, T_i$$

where T_i is in energy units (T_i is the product of Boltzmann's constant and the temperature in degrees Kelvin), and assume thermal conductivities high enough such that T_i is constant and hence

$$\nabla P_i = T_i \nabla n \tag{4.14}$$

Then

$$\nabla\phi_P = \frac{-\Sigma_{p1}}{\Sigma_{p1} + \Sigma_{p2}} \frac{T_{i1}\nabla n_1}{n_1 e}$$

The velocity in level 1 resulting from the combined action of ∇P_i and ϕ_P is

$$\underline{v}_{i1P} = \left[\frac{\nu_{in}}{\Omega_i} R_i \frac{c}{e|B|} \left(- e\nabla\phi_P - T_i \frac{\nabla n}{n}\right)\right]_1$$

$$+ \left[R_i \frac{c}{eB} \left(- e\nabla\phi_P - T_i \frac{\nabla n}{n}\right)\right]_1 \times \hat{z} \qquad (4.15)$$

Now

$$\left(- e\nabla\phi_P - T_i \frac{\nabla n}{n}\right)_1$$

$$= T_{i1} \frac{\nabla n_1}{n_1} \left(\frac{\Sigma_{p1}}{\Sigma_{p1} + \Sigma_{p2}} - 1\right)$$

$$= - T_{i1} \frac{\nabla n_1}{n_1} \left(\frac{\Sigma_{p2}}{\Sigma_{p1} + \Sigma_{p2}}\right) \qquad (4.16)$$

Thus

$$\underline{v}_{i1P} = \frac{-\Sigma_{p2}}{\Sigma_{p1} + \Sigma_{p2}} \left[\left(\frac{\nu_{in}}{\Omega_i} R_i \frac{c}{e|B|} T_i \frac{\nabla N}{N}\right)_1\right.$$

$$\left. + \left(R_i \frac{c}{eB} T_i \frac{\nabla N}{N}\right)_1 \times \hat{z}\right] \qquad (4.17)$$

Note we have used $\frac{\nabla n}{n} = \frac{\nabla N}{N}$.

It is convenient to divide $\underline{v}_{i1P}$ into two parts:

$$\underline{v}_{i1P} = \underline{v}_{D1} + \underline{v}_{S1}$$

with the subscripts i and P suppressed but understood.

$$\underline{v}_{D1} = - \frac{\Sigma_{p2}}{\Sigma_{p1} + \Sigma_{p2}} \left(\frac{\nu_{in}}{\Omega_i} R_i \frac{c}{e|B|} T_i \frac{\nabla N}{N}\right)_1 \tag{4.18}$$

$$\underline{v}_{S1} = - \frac{\Sigma_{p2}}{\Sigma_{p1} + \Sigma_{p2}} \left(R_i \frac{c}{eB} T_i \frac{\nabla N}{N}\right)_1 \times \hat{z} \tag{4.19}$$

That $\underline{v}_{S1}$ represents shear flow at plasma gradients can be seen by noting that the velocity is always perpendicular to ∇N, and is largest where $\frac{\Sigma_{p2}}{\Sigma_{p1} + \Sigma_{p2}} \frac{\nabla N}{N}$ is a maximum, decaying in magnitude away from the region. The quantity $\underline{v}_S$ is of interest because it is a shear flow and hence may be stabilizing in certain cases (see Perkins and Doles [1975], Huba et al. [1982]). We do not consider the effects of $\underline{v}_S$ further in this paper except to note that for the special case of a uniform layer 2 being considered here, $\nabla \cdot \underline{v}_{S1} = 0$ and $\nabla N_1 \cdot \underline{v}_{S1} = 0$ which together imply $\nabla \cdot (N_1 v_{S1}) = 0$, which is to say that $\underline{v}_{S1}$ has no effect on the time evolution of N_1. Since this breaks the feedback loop, it is difficult to see how a shear stabilization mechanism could be active in this case.

A consideration of $\underline{v}_D$ is really the heart of this paper. The quantity $\underline{v}_D$ is the source for ion diffusion in level 1. More importantly, it is the source for the diffusion of the total integrated Pedersen and Hall conductivities if level 2 is sufficiently incompressible (i.e., if ν_{in}/Ω_i in level 2 is sufficiently small), as we will show. Let us look at the effect of $\underline{v}_D$ on the ion continuity equation for level 1:

$$\frac{\partial N_1}{\partial t} = - \nabla \cdot (N_1 \underline{v}_{D1})$$

$$= + \nabla \cdot \left[\frac{\Sigma_{p2}}{\Sigma_{p1} + \Sigma_{p2}} \left(\frac{\nu_{in}}{\Omega_i} R_i \frac{c}{e|B|} T_i \nabla N\right)_1\right] \tag{4.20}$$

This is just a diffusion equation for N_1 with diffusion coefficient

$$D_o = \frac{\Sigma_{p2}}{\Sigma_{p1} + \Sigma_{p2}} \left(\frac{\nu_{in}}{\Omega_i} R_i \frac{c}{e|\Sigma|} T_i\right)_1 \tag{4.21}$$

(It should be noted that this diffusion coefficient is similar to that derived by Goldman et al., 1976, and Vickrey and Kelley, 1982.)

For a barium cloud (level 1) at 180 km altitude we take $T_i \sim 1000^o$ K, $\frac{\nu_{in}}{\Omega_i} \sim 0.06$, B = 0.5 g, and get

$$D_o = \frac{\Sigma_{p2}}{\Sigma_{p1} + \Sigma_{p2}} (100 \text{ m}^2/\text{sec}) \tag{4.22}$$

In the less dense regions of the barium cloud where Σ_{p1} is small compared to Σ_{p2}, the ion diffusion coefficient is quite large indeed. By contrast ambipolar diffusion rates induced by electron-ion and electron-neutral collisions yield diffusion coefficients on the order of 1 m^2/sec. Thus our neglect of these collision terms seems justified. Unfortunately, N_1 is not the relevant quantity if one is interested in the effect of $\underline{v_D}$ on barium cloud dynamics. A look at Eq. (4.10) will convince the reader that if one wants to affect the time evolution of ϕ_E, the quantity which determines the bifurcation process, it is necessary to change the quantities $\Sigma_p \equiv \Sigma_{p1} + \Sigma_{p2}$ and $\Sigma_h \equiv \Sigma_{h1} + \Sigma_{h2}$, the total field line integrated Pedersen and Hall conductivities. Again we assume an initially uniform distribution of Σ_{p2} and N_2. We can only show the effects of $\underline{v_D}$ in the first instant of time here. Once images form in level 2, the problem yields only to numerical techniques. We need the velocity $\underline{v_{D2}}$ in level 2.

$$\underline{v}_{D2} = \left(\frac{\nu_{in}}{\Omega_i} R_i\right)_2 \frac{c}{e|B|} \frac{\Sigma_{p1}}{\Sigma_{p1} + \Sigma_{p2}} \left(T_{i1} \frac{\nabla N_1}{N_1}\right) \tag{4.23}$$

As a check, let us see the effect on $(N_1 + N_2)$

$$\frac{\partial N_2}{\partial t} = - \nabla \cdot (N_2 \underline{v}_{D2})$$

$$= - \nabla \cdot \left(\Sigma_{p2} e^{-2} \frac{\Sigma_{p1}}{\Sigma_{p1} + \Sigma_{p2}} \left(T_{i1} \frac{\nabla N_1}{N_1}\right)\right) \tag{4.24}$$

$$\frac{\partial N_1}{\partial t} = - \nabla_1 (N_1 \underline{v}_{D1})$$

$$= + \nabla \cdot \left(\frac{\Sigma_{p2}}{\Sigma_{p1} + \Sigma_{p2}} \Sigma_{p1} e^{-2} T_{i1} \frac{\nabla N_1}{N_1}\right)$$

$$= - \frac{\partial N_2}{\partial t} \tag{4.25}$$

So we see that

$$\frac{\partial (N_1 + N_2)}{\partial t} = 0 \tag{4.26}$$

which when combined with quasi-neutrality, is simply a statement that electrons can't diffuse. This is consistent with our neglect of electron-ion and electron-neutral collisions.

Now let us look at the effect of $\underline{v}_D$ on $\Sigma_p = \Sigma_{p1} + \Sigma_{p2}$. A similar analysis can be performed for Σ_h with similar results. However the bifurcation effects of Σ_h are small compared to those of Σ_p, and we shall not consider them here.

$$\frac{\partial \Sigma_{p1}}{\partial t} = \left(\frac{\nu_{in}}{\Omega_i} R_i\right)_1 \frac{ce}{|B|} \frac{\partial N_1}{\partial t} = \nabla \cdot \left(\underline{v}_{D1} \Sigma_{p1}\right) \tag{4.27}$$

$$\frac{\partial \Sigma_{p2}}{\partial t} = \left(\frac{\nu_{in}}{\Omega_i} R_i\right)_2 \frac{ce}{|B|} \frac{\partial N_2}{\partial t} = \nabla \cdot \left(\underline{v}_{D2} \Sigma_{p2}\right) \tag{4.28}$$

but

$$\frac{\partial N_1}{\partial t} = -\frac{\partial N_2}{\partial t} = -\frac{|B|}{ce} \left(\frac{\nu_{in}}{\Omega_i} R_i\right)_1^{-1} \frac{\partial \Sigma_{p2}}{\partial t} \tag{4.29}$$

$$\frac{\partial \Sigma_{p1}}{\partial t} = -\frac{\left(\frac{\nu_{in}}{\Omega_i} R_i\right)_1}{\left(\frac{\nu_{in}}{\Omega_i} R_i\right)_2} \frac{\partial \Sigma_{p2}}{\partial t} \tag{4.30}$$

$$\frac{\partial \left(\Sigma_{p1} + \Sigma_{p2}\right)}{\partial t} = \frac{\partial \Sigma_{p1}}{\partial t} \left[1 - \left(\frac{\nu_{in}}{\Omega_i} R_i\right)_2 / \left(\frac{\nu_{in}}{\Omega_i} R_i\right)_1\right] \tag{4.31}$$

Now

$$\frac{\partial \Sigma_{p1}}{\partial t} = -\nabla_{\perp} \cdot \left(\underline{v}_{D1} \Sigma_{p1}\right) \tag{4.32}$$

We note that in Eq. (4.18) we may set $\nabla N_1/N_1 = \nabla \Sigma_{p1}/\Sigma_{p1}$ so that

$$\frac{\partial \Sigma_{p1}}{\partial t} = \nabla \cdot \left[\frac{\Sigma_{p2}}{\Sigma_{p1} + \Sigma_{p2}} \left(\frac{\nu_{in}}{\Omega_i} R_i \frac{c}{e|B|} T_i\right)_1 \nabla \Sigma_{p1}\right] \tag{4.33}$$

Now since

$$\nabla \Sigma_{p2} = 0 \tag{4.34}$$

we have

$$\nabla(\Sigma_{p1} + \Sigma_{p2}) = \nabla\Sigma_{p1} \tag{4.35}$$

and

$$\frac{\partial(\Sigma_{p1} + \Sigma_{p2})}{\partial t} = \nabla_{\perp} \cdot \left[\left(1 - (\nu_{in}R_i/\Omega_i)_2/(\nu_{in}R_i/\Omega_i)_1\right)\left(\frac{\Sigma_{p2}}{\Sigma_{p1} + \Sigma_{p2}}\right)\right.$$

$$\left.\left(\frac{\nu_{in}}{\Omega_i} R_i \frac{c}{eB} T_i\right)_1 \nabla(\Sigma_{p1} + \Sigma_{p2})\right] \tag{4.36}$$

so we see that for Σ_p we again have a diffusion equation, but this time our nominal 100 m^2/sec diffusion coefficient is not only multiplied by $\Sigma_{p2}/(\Sigma_{p1} + \Sigma_{p2})$, reducing its effectiveness in the dense portions of the cloud, but it is further multiplied by the factor F where

$$F = 1 - \frac{(\nu_{in}R_i/\Omega_i)_2}{(\nu_{in}R_i/\Omega_i)_1} \tag{4.37}$$

Note that if $\nu_{in}R_i/\Omega_i$ is the same for both layers, the diffusion is reduced to zero. Furthermore, if $(\nu_{in}R_i/\Omega_i)_2 > (\nu_{in}R_i/\Omega_i)_1$ (a compressible background plasma, e.g., an E region) the diffusion coefficient is negative. That is, gradients in Σ_p will actually be steepened, rather than smoothed. For this reason we conclude that unless some rather fast recombination chemistry is taking place in the E region, the presence of a background E region is destabilizing, in accord with the findings of Francis and Perkins [1975].

The opposite extreme of $(\nu_{in}R_i/\Omega_i)_2 << (\nu_{in}R_i/\Omega_i)$ (background F region ionosphere) is more interesting since it closely approximates the conditions of most barium releases. It also yields the full nominal 100 m^2/sec diffusion coefficient, since $F \approx 1.0$, giving us some hope of

stopping the bifurcation process at scale sizes of hundreds of meters. Note that in this case the diffusion rate for Σ_p is the same as that for N_1. Also note that the case of $(\nu_{in}R_i/\Omega_i)_2$ small is the case where the Pedersen mobility and hence compressibility of the background is extremely low, meaning that only minimal images will be formed. It is a good approximation to take Σ_{p2} to be uniform for all time. One might well ask how this is possible given that the electrons can't diffuse, and that the barium ions are being allowed to diffuse in level 1. The answer is that there <u>are</u> (small) images: the electrons lost to a field line in level 1 are "soaked up" on the same field line in level 2. But the number of electrons N_2 in level 2 is <u>extremely</u> large. (N_2 must be large in order to contribute a significant Pedersen conductivity and yet have small $\nu_{in}R_i/\Omega_i$ (see Eq. 2.24)). Thus the electrons that are soaked up in level 2 induce only an extremely small percentage change in Σ_{p2}.

5. Diffusion Characteristics for a Simplified Two-level Model with a Nearly Incompressible Background Layer

In the last section we demonstrated that when the background ionosphere (layer 2) is nearly incompressible ($(\nu_{in}R_i/\Omega_i)_2$ is small) then the primary effect of a finite barium ion temperature is to introduce into the continuity equation for both N_1 and for Σ_p a diffusion term with diffusion coefficient D_o given by Eq. (4.21). For parameters appropriate to a barium cloud at 180 km altitude we get Eq. (4.22):

$$D_o = \frac{\Sigma_{p2}}{\Sigma_{p1} + \Sigma_{p2}} (100 \text{ m}^2/\text{sec}) \qquad (4.22)$$

Since level 2 is nearly incompressible, we may regard Σ_{p2} as a constant.

Since it is proportional to N_1, the integrated barium cloud density, Σ_{p1} is larger in the center of the cloud and decays toward zero at the cloud edges. This means that the diffusion coefficient approaches 100 m^2/sec near the cloud edges, but may be considerably less than that value near the cloud center if $\Sigma_{p1} \gg \Sigma_{p2}$.

Previous attempts to explain the persistence of scale sizes of hundreds of meters for long periods of time after barium releases have inevitably encountered the following problems: 1) The diffusion coefficients required to stop the bifurcation of plasma clouds several hundred meters in diameter were higher than one could explain theoretically; 2) assuming the existence of such large (ordinary) diffusion coefficients, their effect would not only be to stop the bifurcation of the cloud, but also to diffuse the cloud away entirely in several minutes. The form of the diffusion coefficient given by Eq. (4.22) would seem to offer us some hope of overcoming both of these problems. Its success depends on the accuracy of the following qualitative picture of barium cloud bifurcation: We postulate a barium cloud such that $\Sigma_{p1} \gtrsim 5\,\Sigma_{p2}$ so that the diffusion well inside the cloud is considerably reduced over that at its edges. We further postulate that bifurcation is a process which, in the absence of diffusion, starts at the edges of barium clouds and works its way inward. Our diffusion then satisfies the needed criteria perfectly: 1) It is very effective at the edges of the cloud, stopping bifurcation before it starts; 2) it is very ineffective at the central core of the cloud, giving it a long lifetime. Note that if this picture is correct then the barium clouds commonly known as large M clouds where

$$M \equiv \frac{\Sigma_{p1} + \Sigma_{p2}}{\Sigma_{p2}} \tag{5.1}$$

will have extremely long lifetimes. In fact for $M \gtrsim 100$, the decay of the core is probably determined by ambipolar diffusion rates. The accuracy of this picture is best determined by numerical simulation techniques, to which we turn in the next section.

6. Numerical Simulations Using a Simplified Two-level Model with a Nearly Incompressible Background Layer

In this section we attempt to answer numerically the question posed in the last section: if we consider a barium cloud whose background conductivity is due primarily to high F region plasma (nearly incompressible plasma), is the diffusion coefficient given by Eq. (4.22) sufficient to stop the bifurcation of that cloud at a diameter of several hundred meters? In order to isolate the effects of this diffusion coefficient, we will make some further simplifications in our two-level model: 1) We assume that N_2 and hence Σ_{p2} remain uniform during all times of interest. This is completely consistent with our assumption of a nearly incompressible background plasma, as discussed at the end of Section 4; 2) We neglect the shear component $\underline{v}_S$ of the pressure-induced ion velocity as defined in Eq. (4.19). Again this is consistent with our assumption of a nearly incompressible background plasma which in turn implies a uniform Σ_{p2}, as shown in the discussion following Eq. (4.19); 3) We neglect the "Hall term" H in Eq. (4.4) and hence in Eq. (4.10). This is a good approximation as long as $\nu_{in}/\Omega_i < 0.1$; 4) We neglect Pedersen convection. That is, for all terms except those causing ion diffusion, we approximate the ion velocity with the electron velocity (see Eq. (6.4)

below). We know from our previous study [Zalesak et. al,, 1983] that the Pedersen mobility of the ions in response to $(\underline{E}_o - \nabla\phi_E)$ can have an effect on the "freezing" phenomenom, and it is our desire to isolate the effects of the pressure-induced diffusion. Hence we neglect ion Pedersen mobility except in the diffusion term.

The final equations to be solved numerically are then

$$\frac{\partial N_1}{\partial t} + \nabla_\perp \cdot (N_1 \underline{v}_1) = \nabla_\perp \cdot (D \nabla N_1) \tag{6.1}$$

$$\frac{\partial N_2}{\partial t} = 0 \tag{6.2}$$

$$\nabla_\perp ((\Sigma_{p1} + \Sigma_{p2}) \nabla_\perp \phi_E) = \underline{E}_o \cdot \nabla_\perp (\Sigma_{p1} + \Sigma_{p2}) \tag{6.3}$$

$$\underline{v}_1 = \frac{c}{B^2} (\underline{E}_o - \nabla\phi_E) \times \underline{B} \tag{6.4}$$

$$D = \frac{\Sigma_{p2}}{\Sigma_{p1} + \Sigma_{p2}} D_{io} \tag{6.5}$$

$$\Sigma_{pk} \equiv N_k \left(\frac{\nu_{in}/\Omega_i}{1+(\nu_{in}/\Omega_i)^2} \right)_k \frac{ce}{|B|} \tag{6.6}$$

The initial conditions for the simulations were as follows

$$\Sigma_{p2} = 1.0 \tag{6.7}$$

$$\Sigma_{p1} = 4.0 \exp\ (-r^4/r_o^4) \tag{6.8}$$

$$r^2 = (x - x_o)^2 + (y - y_o)^2 \tag{6.9}$$

$$r_o = (250\ \text{m})\ (1 + 0.001 \sin 8\theta) \tag{6.10}$$

$$\theta = \arctan\ [(y-y_o)/(x - x_o)] \tag{6.11}$$

$$B = 0.5\ \text{gauss} \tag{6.12}$$

$$cE_o/B = 100\ \text{m/sec} \tag{6.13}$$

where x_o and y_o are the coordinates of the cloud center and the $\underline{E}_o \times \underline{B}$ velocity (cE_o/B) is in the negative y direction.

The above equations are solved numerically on a finite difference grid in an x-y cartesian geometry perpendicular to the magnetic field, which is assumed to be aligned along the z-axis. The 83 x 60 grid is stretched in all four directions, with the central 56 x 32 portion of the grid, which is centered on the steepening backside of the cloud, having a grid spacing of 10 m in both directions. The grid stretching allows the boundaries to be placed 4 km away from the edges of the central uniform mesh in all directions. The potential equation (6.3) is solved using a vectorized incomplete Cholesky conjugate gradient algorithm due to Hain (1980), which is an extension of the algorithm of Kershaw (1978). The continuity equation (6.1) is integrated forward in time using the fully multidimensional flux-corrected transport algorithms of Zalesak [1979].

In Figure 3 we show isodensity contours of Σ_{pl} for the initial conditions for all of the calculations we shall show. We have performed three calculations, varying the value of D_{io} from zero up to the physically realistic value of 100 m^2/sec. The purpose of this sequence is to show first that the diffusion does have an effect on the evolution of the cloud,

and second to show that this effect is much larger than that due to any numerical diffusion which may be present in the calculations. In Figure 4 we show the results for $D_{io} = 0$. Note that even at the very early time of 14 seconds, bifurcation has already started. By 24 seconds, the main portion of the cloud has completely sheared in two. In Figure 5, we show the results for $D_{io} = 25\ m^2/sec$, one fourth of the physically realistic value. The development of the cloud has slowed considerably, showing that even at one fourth its physically realistic value, the physical diffusion is dominating the effects of whatever numerical diffusion may be present. At 14 seconds the cloud has not clearly begun to bifurcate. At 25 seconds, bifurcation has occurred, but is qualitatively and quantitatively different from that which took place when $D_{io} = 0$. In Figure 6 we show the evolution of the cloud with the full, physically realistic value for D_{io} of 100 m^2/sec. Bifurcation has now been halted. Rather, the cloud evolves into a streamlined "bullet" or "tadpole" shape in time, and then undergoes a slow diffusive decay. Even at the latest time calculated, 75 sec, there is no hint whatsoever of imminent bifurcation. Noting that for this cloud $M = (\Sigma_{p1} + \Sigma_{p2})/\Sigma_{p2}$ is 5 in the center of the cloud, which yields an effective diffusion coefficient of 20 m^2/sec there. This is still enough to result in substantial decay of the central core on time scales of minutes. Clouds with larger values of M in their centers would of course be longer-lived.

7. Conclusions and Future Work

The primary conclusion of this paper can be stated simply: Under realistic ionospheric conditions (where the plasma cloud couples to an incompressible background i.e., in F region), barium striations hundreds of meters in diameter can be long-lived, quasi-stable, non-bifurcating structures. These structures may resemble "tadpoles", with a dense head, steep density gradients at the front, and a long, less dense tail. If what one means by the term "freezing" is the above phenomenon, then we have shown that freezing does indeed exist.

The next obvious step is to test some of the approximations we have made in our preliminary numerical simulation model. Pedersen convection should be put back into the model, as well as the "Hall terms" in the potential equation. Finite images should be accounted for. Also we would like to test the combined effect of the presence of both a relatively incompressible F region background and a compressible E region on the dynamics of the cloud. Recombination chemistry must be included in this E region if it is to be modeled accurately (see Vickery and Kelley, 1982].

Another of our approximations which should be studied in detail is that the barium cloud and background ionosphere are being driven by an externally imposed electric field, or equivalently, by a neutral wind which doesn't vary in altitude. Were we to address an altitude-dependent neutral wind as a driver, some of our simple results would become less so. The most important factor would be that one could no longer argue that the bifurcation of the cloud depended only on Σ_{p1} and Σ_{p2}, since the potential equation (4.10) would then contain terms which depended explicitly on N_1 and N_2. Although this would not change the results for the incompressible background ionosphere considered here, it would appear to allow for the

possibility of this end-shorting-induced diffusion being an effective bifurcation inhibiting mechanism even when the background ionosphere is compressible. We shall consider this case in our future work in this area.

It is also clear that we must address the validity of the perfect mapping of the electrostatic potential along B. Given that we are now dealing with structures only a few hundred meters in diameter, with gradient scale lengths of a few tens of meters, it seems likely that we will have to deal with the question of how far the polarization field produced by the barium cloud maps along the magnetic field (Goldman et. al, 1976, Glassman and Sperling, 1983). One possible effect might be that the effective value of M would be increased, since the barium cloud could no longer "see" background plasma that was far from the cloud position along B.

Acknowledgments

This research was sponsored by the Defense Nuclear Agency.

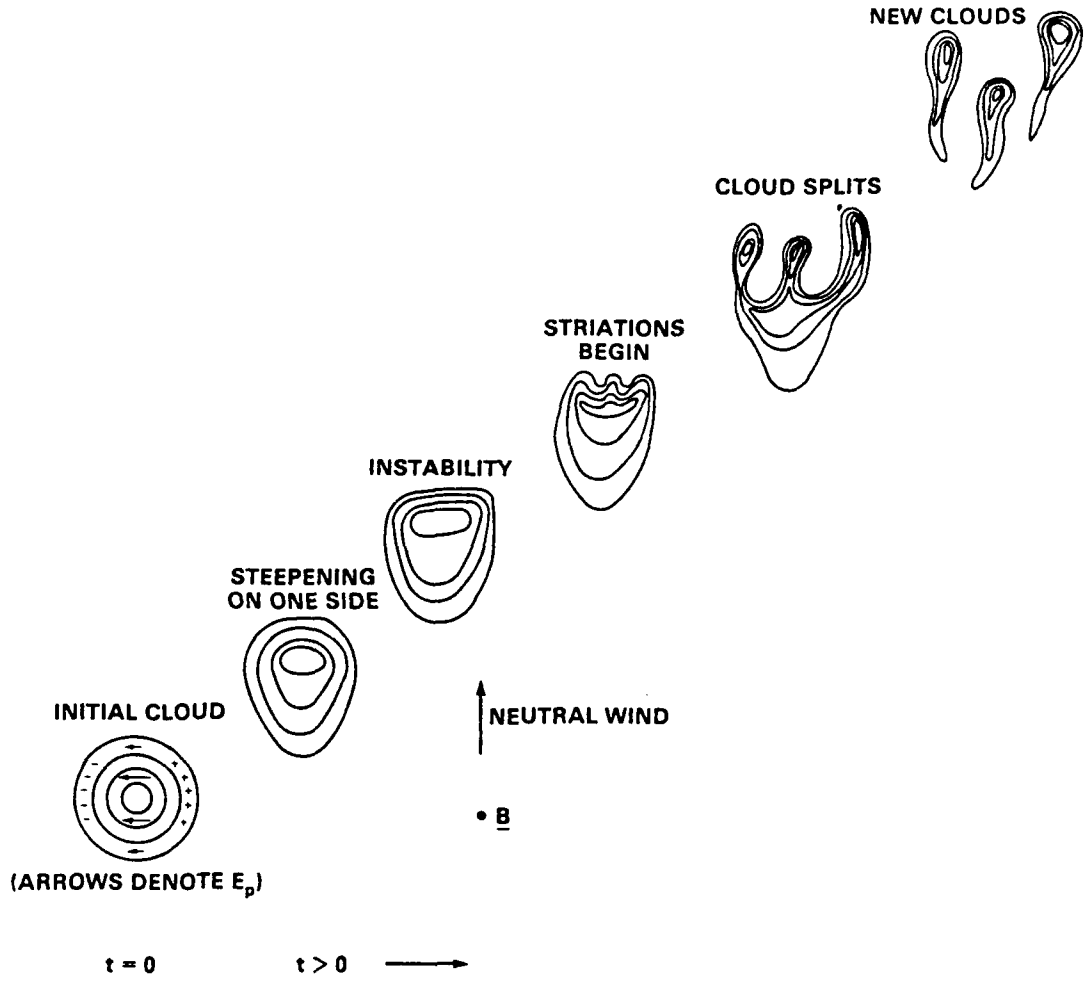

Figure 1. Sketch of the time evolution of a typical barium cloud in a plane perpendicular to the magnetic field, subject to an upward directed neutral wind or equivalently to a rightward directed external electric field. Lines demarking the cloud denote plasma density contours, with the highest plasma density in the center of cloud.

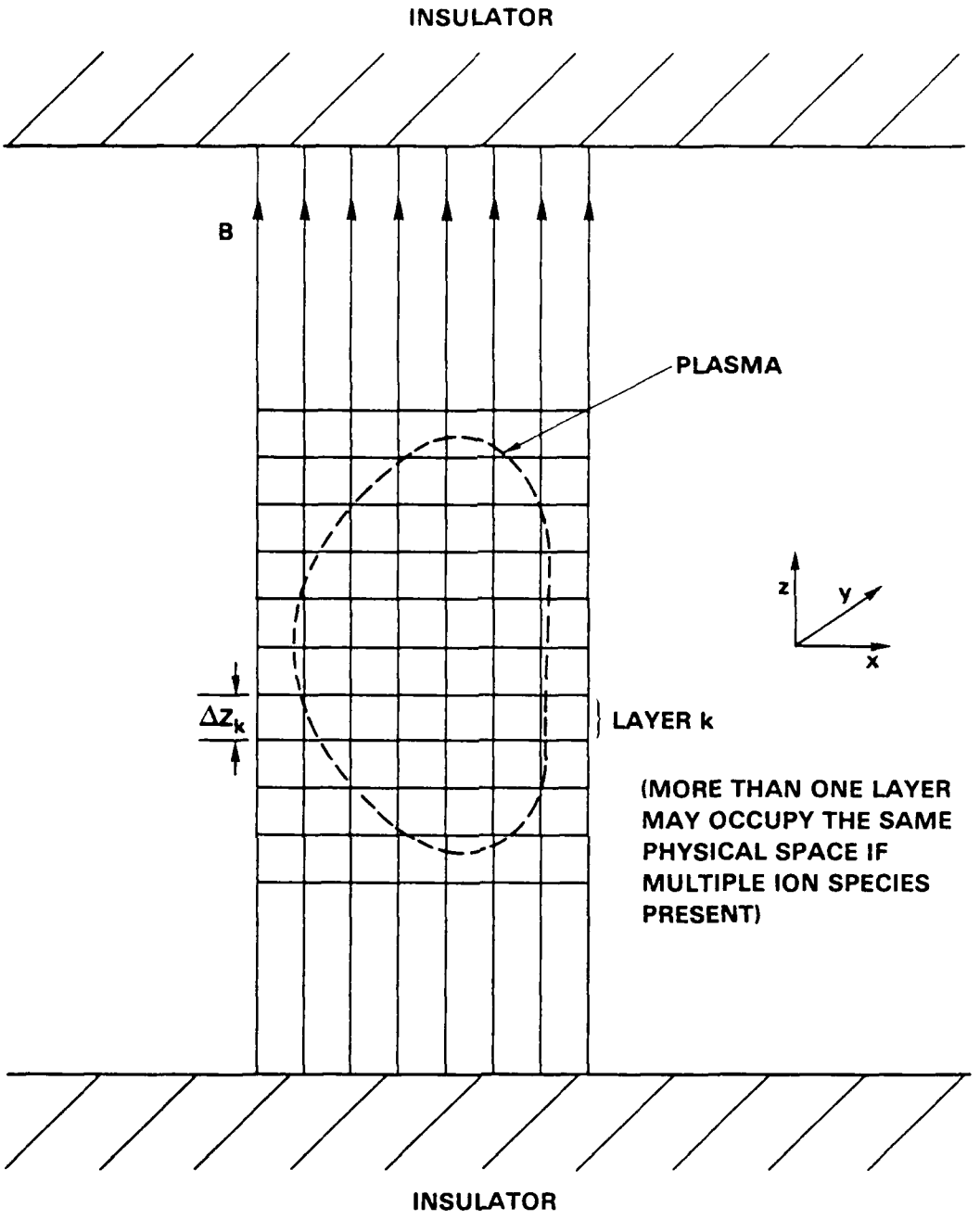

Figure 2. Model of plasma and magnetic field geometry used in this paper. Field lines terminate on insulators at $z = \pm \infty$. Plasma is divided into "layers" along z for mathematical and numerical treatment. Each layer consists of a single ion species and its associated electrons. Multiple collocated ion species are treated by having multiple collocated "layers".

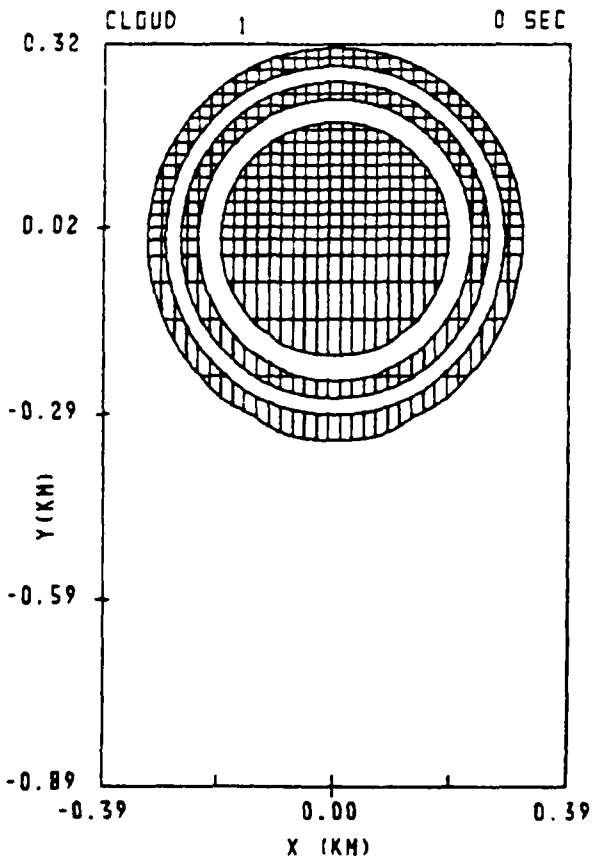

Figure 3. Isodensity contours, with areas between alternate contours shown cross-hatched, for the barium cloud used for the three numerical simulations shown in this paper. The center of the cloud is located at the point (0,0). The boundaries in x are located at $\pm$ 4.9 km. The boundaries in y are located at -4.0 km and +5.3 km respectively. The cross-hatching is done at every other grid line, so that one rectangle of cross hatching represents a 2 x 2 array of computational cells. Contours for this and all other plots in this paper are drawn at values for Σ_{pl} of 0.31, 0.71, 1.24, 1.92, and 2.82 (logarithmic spacing for <u>total</u> Pedersen conductivity).

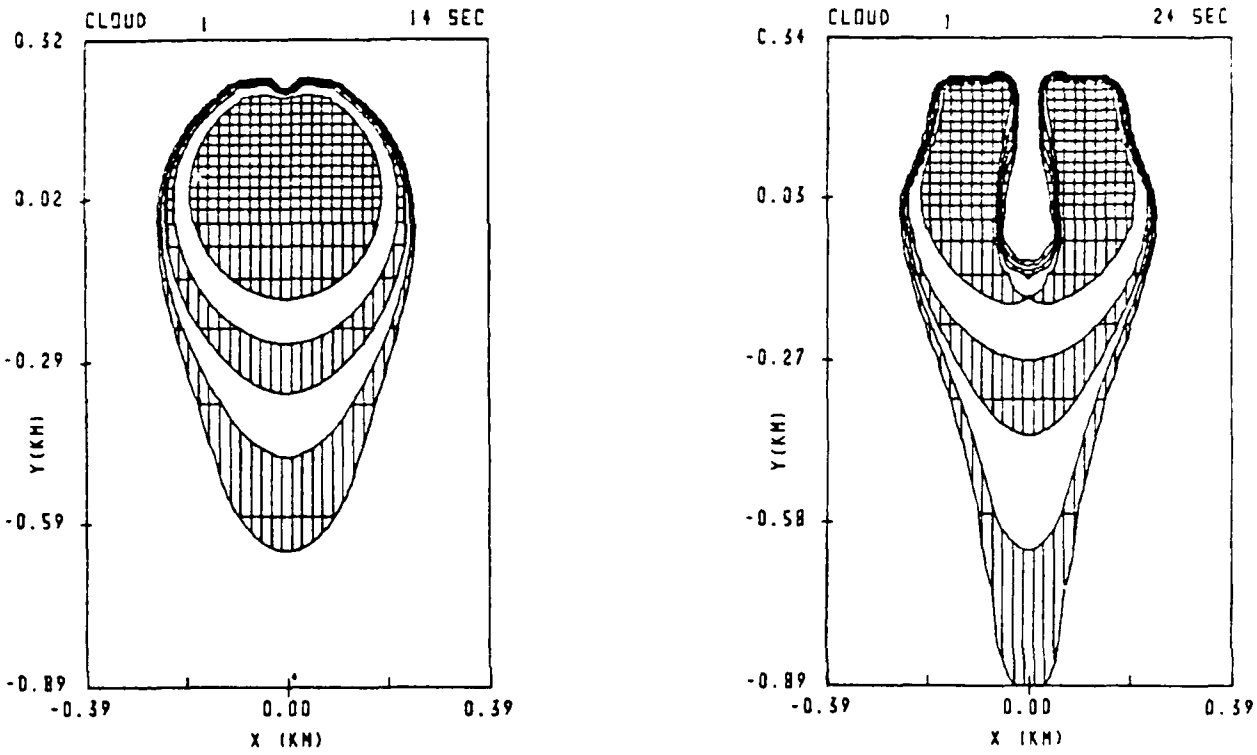

Figure 4. Time evolution of the cloud depicted in Figure 3 for the case $D_{io} = 0$. Shown are isodensity contours at a) 14 sec, b) 24 sec. Contour values are as given in Figure 3.

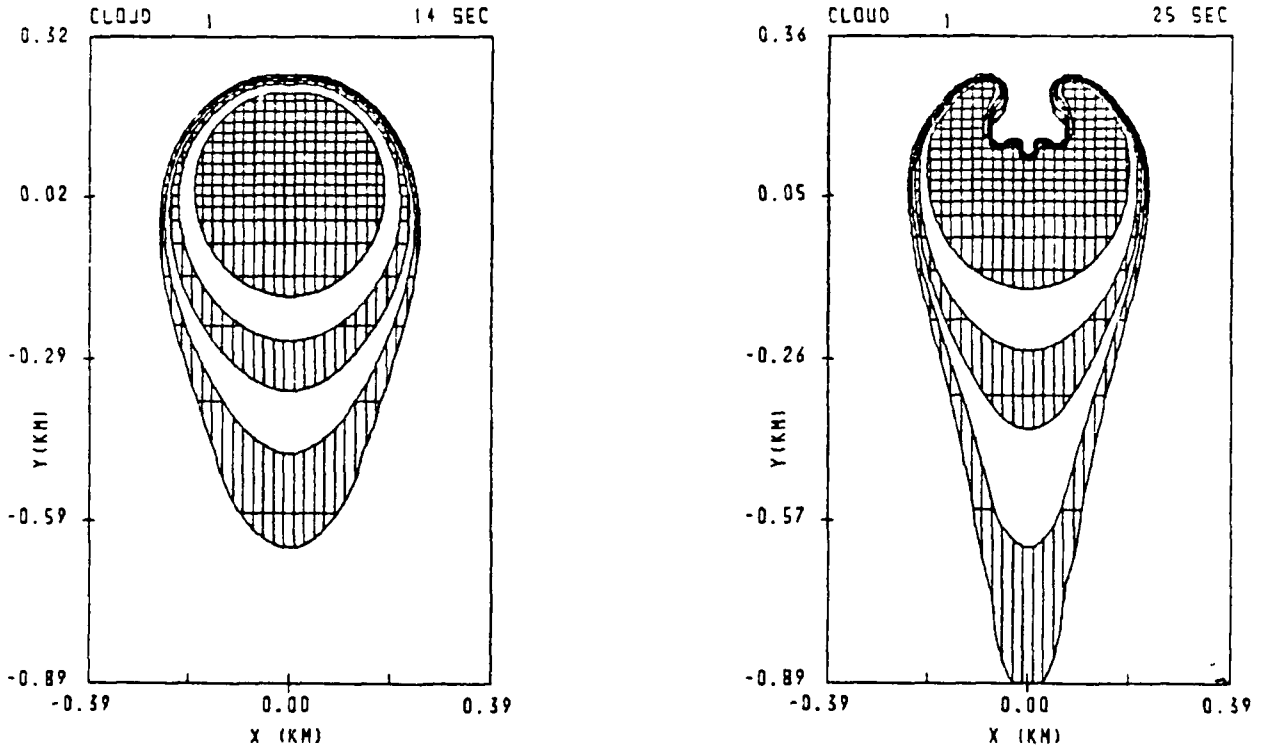

Figure 5. Time evolution of the cloud depicted in Figure 3 for the case $D_{io} = 25\ m^2/sec$. Shown are isodensity contours at a) 14 sec, b) 24 sec. Contour values are as given in Figure 3.

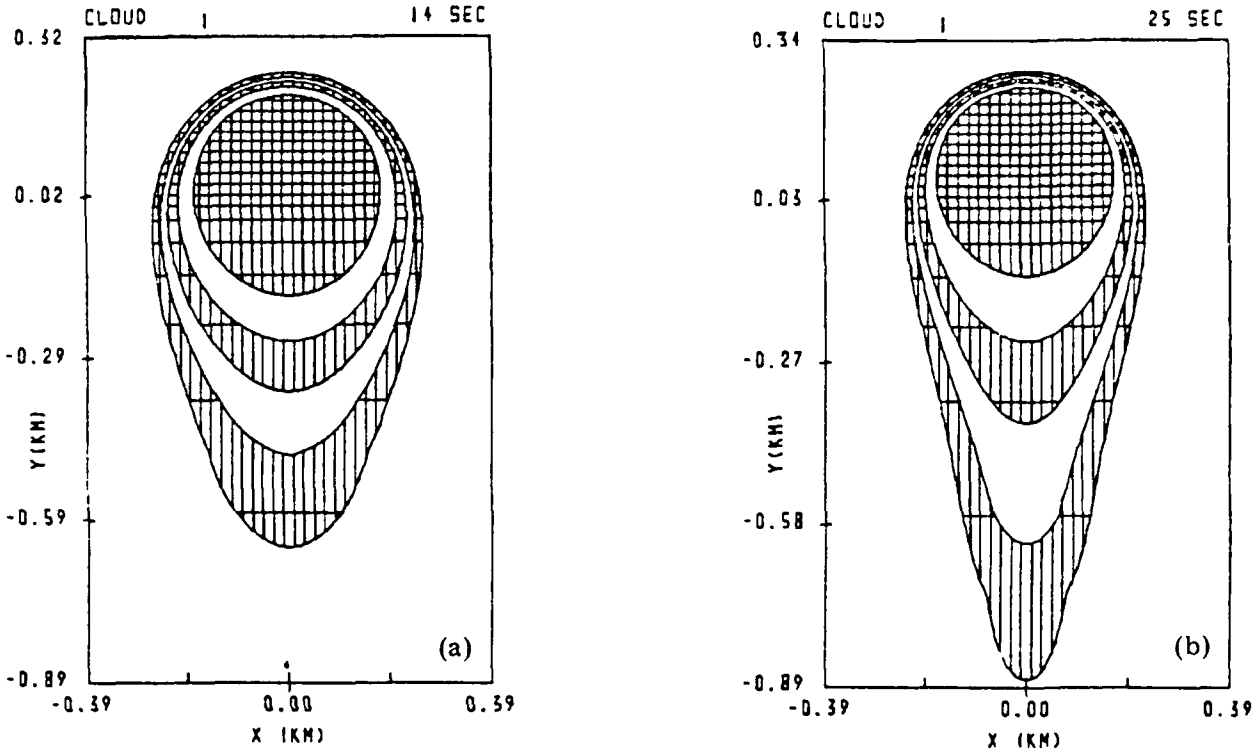

Figure 6. Time evolution of the cloud depicted in Figure 3 for the case D_{io} = 100 m^2/sec (the physically realistic case). Shown are isodensity contours at a) 14 sec, b) 25 sec, c) 39 sec, d) 50 sec, e) 64 sec, f) 75 sec.

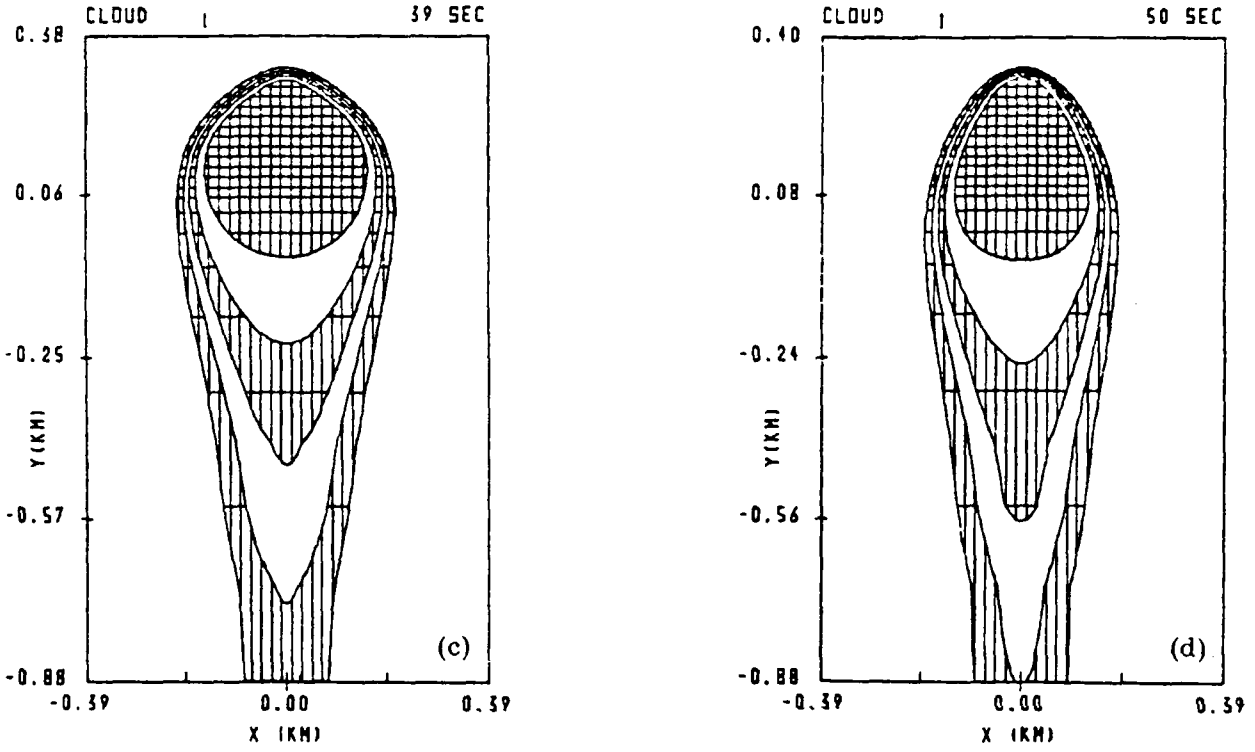

Figure 6, cont'd. Time evolution of the cloud depicted in Figure 3 for the case D_{io} = 100 m^2/sec (the physically realistic case). Shown are isodensity contours at a) 14 sec, b) 25 sec, c) 39 sec, d) 50 sec, e) 64 sec, f) 75 sec.

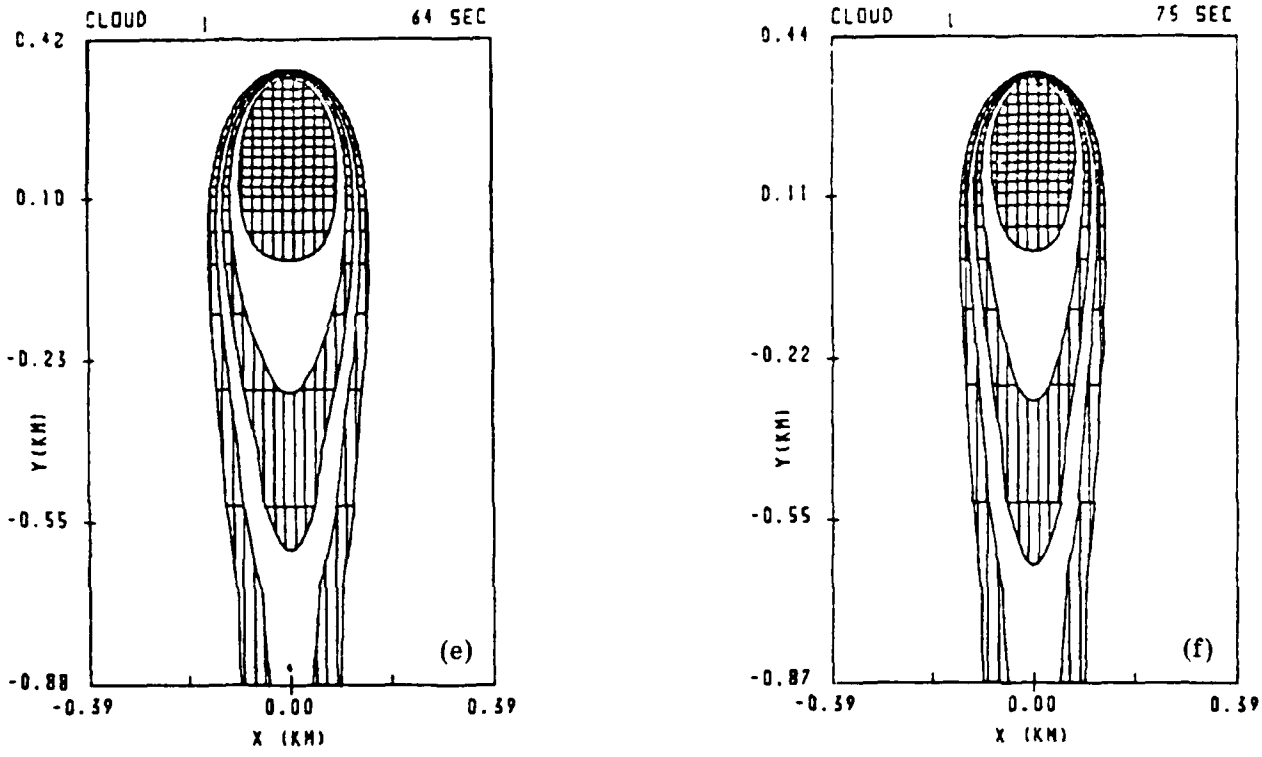

Figure 6, cont'd. Time evolution of the cloud depicted in Figure 3 for the case D_{io} = 100 m^2/sec (the physically realistic case). Shown are isodensity contours at a) 14 sec, b) 25 sec, c) 39 sec, d) 50 sec, e) 64 sec, f) 75 sec.

References

Fedder, J.A., Conductivity formulas for the disturbed ionosphere, Memo Report 4329, Naval Res. Lab., Washington, D.C., Sept., 1980. ADA089 374

Francis, S.H., and F.W. Perkins, Determination of striation scale sizes for plasma clouds in the ionosphere, J. Geophys. Res., 80, 3111, 1975.

Glassman, A.J. and J.L. Sperling, Electromagnetic theory of collisional interchange instabilities, J. Geophys. Res., 88, 10091,1983.

Goldman, S.R., L. Baker, S.L. Ossakow, and A.J. Scannapieco, Striation formation associated with barium clouds in an inhomogeneous ionosphere, J. Geophys. Res., 81, 5097, 1976.

Hain, K., A non-recursive incomplete Cholesky decomposition method for the solution of linear equations with a sparse matrix, Memo Report 4264, Naval Res. Lab., Washington, D.C., June 1980. ADA087005

Huba, J.D., S.L. Ossakow, P. Satyanarayana, and P.N. Guzdar, Linear theory of the E x B instability with an inhomegeneous electric field, J. Geophys. Res., 88, 425, 1983.

Kershaw, D.S., The incomplete Cholesky-conjugate gradient method for the iterative solution of systems of linear equations,J. Comput. Phys. 26, 43, 1978.

McDonald, B.E., Ossakow, S.L., Zalesak, S.T., and Zubusky, N.J., "Scale sizes and lifetimes of F region plasma cloud striations as determined by the condition of marginal stability," J. Geophys. Res., 86, 5775, 1981.

Ossakow, S.L., Ionospheric irregularities, Rev. Geophys. Space Phys., 17, 521, 1979.

Ossakow, S.L., S.T. Zalesak, and M.J. Keskinen, A plausible hypothesis for striation freezing in ionospheric plasma clouds, Memo Report 4597, Naval Res. Lab., Washington, D.C., Aug. 1981.

Ossakow, S.L., M.J. Keskinen and S.T. Zalesak, Ionospheric irregularity physics modelling, AIAA Pap. 82-0147, 1982.

Perkins, F.W., and J.H. Doles III, Velocity shear and the E x B instability, J. Geophys Res., 80, 211, 1975.

Scannapieco, A.J., S.L. Ossakow, S.R. Goldman, and J.M. Pierre, Plasma cloud late time striation spectra, J. Geophys. Res., 81, 6037, 1976.

Shiau, J.N., and A. Simon, Barium cloud growth and striation in a conducting background, J. Geophys. Res., 79, 1895, 1974.

Vickrey, J.F., and M.C. Kelley, The effects of a conducting E layer on classical F region cross-field plasma diffusion, J. Geophys. Res., 87 4461, 1982.

Zalesak, S.T., Fully multidimensional flux-corrected transport algorithms for fluids, J. Comp. Phys., 31, 335, 1979.

Zalesak, S.T., J.A. Fedder, and S.L. Ossakow, Analysis and numerical simulation of the effect of ion Pedersen mobility on ionospheric barium clouds, J. Geophys. Res., 88, 8003, 1983.

DISTRIBUTION LIST

DEPARTMENT OF DEFENSE

ASSISTANT SECRETARY OF DEFENSE
COMM, CMD, CONT 7 INTELL
WASHINGTON, D.C. 20301

DIRECTOR
COMMAND CONTROL TECHNICAL CENTER
PENTAGON RM BE 685
WASHINGTON, D.C. 20301
01CY ATTN C-650
01CY ATTN C-312 R. MASON

DIRECTOR
DEFENSE ADVANCED RSCH PROJ AGENCY
ARCHITECT BUILDING
1400 WILSON BLVD.
ARLINGTON, VA. 22209
01CY ATTN NUCLEAR MONITORING RESEARCH
01CY ATTN STRATEGIC TECH OFFICE

DEFENSE COMMUNICATION ENGINEER CENTER
1860 WIEHLE AVENUE
RESTON, VA. 22090
01CY ATTN CODE R410
01CY ATTN CODE R812

DEFENSE TECHNICAL INFORMATION CENTER
CAMERON STATION
ALEXANDRIA, VA. 22314
02CY

DIRECTOR
DEFENSE NUCLEAR AGENCY
WASHINGTON, D.C. 20305
01CY ATTN STVL
04CY ATTN TITL
01CY ATTN DDST
03CY ATTN RAAE

COMMANDER
FIELD COMMAND
DEFENSE NUCLEAR AGENCY
KIRTLAND, AFB, NM 87115
01CY ATTN FCPR

DEFENSE NUCLEAR AGENCY
SAO/DNA
BUILDING 20676
KIRTLAND AFB, NM 87115
01CY D.C. THORNBURG

DIRECTOR
INTERSERVICE NUCLEAR WEAPONS SCHOOL
KIRTLAND AFB, NM 87115
01CY ATTN DOCUMENT CONTROL

JOINT CHIEFS OF STAFF
WASHINGTON, D.C. 20301
01CY ATTN J-3 WWMCCS EVALUATION OFFICE

DIRECTOR
JOINT STRAT TGT PLANNING STAFF
OFFUTT AFB
OMAHA, NB 68113
01CY ATTN JLTW-2
01CY ATTN JPST G. GOETZ

CHIEF
LIVERMORE DIVISION FLD COMMAND DNA
DEPARTMENT OF DEFENSE
LAWRENCE LIVERMORE LABORATORY
P.O. BOX 808
LIVERMORE, CA 94550
01CY ATTN FCPRL

COMMANDANT
NATO SCHOOL (SHAPE)
APO NEW YORK 09172
01CY ATTN U.S. DOCUMENTS OFFICER

UNDER SECY OF DEF FOR RSCH & ENGRG
DEPARTMENT OF DEFENSE
WASHINGTON, D.C. 20301
01CY ATTN STRATEGIC & SPACE SYSTEMS (OS)

WWMCCS SYSTEM ENGINEERING ORG
WASHINGTON, D.C. 20305
01CY ATTN R. CRAWFORD

COMMANDER/DIRECTOR
ATMOSPHERIC SCIENCES LABORATORY
U.S. ARMY ELECTRONICS COMMAND
WHITE SANDS MISSILE RANGE, NM 88002
01CY ATTN DELAS-EO F. NILES

DIRECTOR
BMD ADVANCED TECH CTR
HUNTSVILLE OFFICE
P.O. BOX 1500
HUNTSVILLE, AL 35807
01CY ATTN ATC-T MELVIN T. CAPPS
01CY ATTN ATC-O W. DAVIES
01CY ATTN ATC-R DON RUSS

PROGRAM MANAGER
BMD PROGRAM OFFICE
5001 EISENHOWER AVENUE
ALEXANDRIA, VA 22333
01CY ATTN DACS-BMT J. SHEA

CHIEF C-E- SERVICES DIVISION
U.S. ARMY COMMUNICATIONS CMD
PENTAGON RM 1B269
WASHINGTON, D.C. 20310
01CY ATTN C- E-SERVICES DIVISION

COMMANDER
FRADCOM TECHNICAL SUPPORT ACTIVITY
DEPARTMENT OF THE ARMY
FORT MONMOUTH, N.J. 07703
01CY ATTN DRSEL-NL-RD H. BENNET
01CY ATTN DRSEL-PL-ENV H. BOMKE
01CY ATTN J.E. QUIGLEY

COMMANDER
U.S. ARMY COMM-ELEC ENGRG INSTAL AGY
FT. HUACHUCA, AZ 85613
01CY ATTN CCC-EMEO GEORGE LANE

COMMANDER
U.S. ARMY FOREIGN SCIENCE & TECH CTR
220 7TH STREET, NE
CHARLOTTESVILLE, VA 22901
01CY ATTN DRXST-SD

COMMANDER
U.S. ARMY MATERIAL DEV & READINESS CMD
5001 EISENHOWER AVENUE
ALEXANDRIA, VA 22333
01CY ATTN DRCLDC J.A. BENDER

COMMANDER
U.S. ARMY NUCLEAR AND CHEMICAL AGENCY
7500 BACKLICK ROAD
BLDG 2073
SPRINGFIELD, VA 22150
01CY ATTN LIBRARY

DIRECTOR
U.S. ARMY BALLISTIC RESEARCH LABORATORY
ABERDEEN PROVING GROUND, MD 21005
01CY ATTN TECH LIBRARY EDWARD BAICY

COMMANDER
U.S. ARMY SATCOM AGENCY
FT. MONMOUTH, NJ 07703
01CY ATTN DOCUMENT CONTROL

COMMANDER
U.S. ARMY MISSILE INTELLIGENCE AGENCY
REDSTONE ARSENAL, AL 35809
01CY ATTN JIM GAMBLE

DIRECTOR
U.S. ARMY TRADOC SYSTEMS ANALYSIS ACTIVITY
WHITE SANDS MISSILE RANGE, NM 88002
01CY ATTN ATAA-SA
01CY ATTN TCC/F. PAYAN JR.
01CY ATTN ATTA-TAC LTC J. HESSE

COMMANDER
NAVAL ELECTRONIC SYSTEMS COMMAND
WASHINGTON, D.C. 20360
01CY ATTN NAVALEX 034 T. HUGHES
01CY ATTN PME 117
01CY ATTN PME 117-T
01CY ATTN CODE 5011

COMMANDING OFFICER
NAVAL INTELLIGENCE SUPPORT CTR
4301 SUITLAND ROAD, BLDG. 5
WASHINGTON, D.C. 20390
01CY ATTN MR. DUBBIN STIC 12
01CY ATTN NISC-50
01CY ATTN CODE 5404 J. GALET

COMMANDER
NAVAL OCCEAN SYSTEMS CENTER
SAN DIEGO, CA 92152
01CY ATTN J. FERGUSON

NAVAL RESEARCH LABORATORY
WASHINGTON, D.C. 20375
01CY ATTN CODE 4700 S. L. Ossakow
26 CYS IF UNCLASS. 1 CY IF CLASS)
01CY ATTN CODE 4701 I Vitkovitsky
01CY ATTN CODE 4780 J. Huba (100
CYS IF UNCLASS, 1 CY IF CLASS)
01CY ATTN CODE 7500
01CY ATTN CODE 7550
01CY ATTN CODE 7580
01CY ATTN CODE 7551
01CY ATTN CODE 7555
01CY ATTN CODE 4730 E. MCLEAN
01CY ATTN CODE 4108
01CY ATTN CODE 4730 B. RIPIN
20CY ATTN CODE 2628

COMMANDER
NAVAL SEA SYSTEMS COMMAND
WASHINGTON, D.C. 20362
01CY ATTN CAPT R. PITKIN

COMMANDER
NAVAL SPACE SURVEILLANCE SYSTEM
DAHLGREN, VA 22448
01CY ATTN CAPT J.H. BURTON

OFFICER-IN-CHARGE
NAVAL SURFACE WEAPONS CENTER
WHITE OAK, SILVER SPRING, MD 20910
01CY ATTN CODE F31

DIRECTOR
STRATEGIC SYSTEMS PROJECT OFFICE
DEPARTMENT OF THE NAVY
WASHINGTON, D.C. 20376
01CY ATTN NSP-2141
01CY ATTN NSSP-2722 FRED WIMBERLY

COMMANDER
NAVAL SURFACE WEAPONS CENTER
DAHLGREN LABORATORY
DAHLGREN, VA 22448
01CY ATTN CODE DF-14 R. BUTLER

OFFICER OF NAVAL RESEARCH
ARLINGTON, VA 22217
01CY ATTN CODE 465
01CY ATTN CODE 461
01CY ATTN CODE 402
01CY ATTN CODE 420
01CY ATTN CODE 421

COMMANDER
AEROSPACE DEFENSE COMMAND/DC
DEPARTMENT OF THE AIR FORCE
ENT AFB, CO 80912
01CY ATTN DC MR. LONG

COMMANDER
AEROSPACE DEFENSE COMMAND/XPD
DEPARTMENT OF THE AIR FORCE
ENT AFB, CO 80912
01CY ATTN XPDQQ
01CY ATTN XP

AIR FORCE GEOPHYSICS LABORATORY
HANSCOM AFB, MA 01731
01CY ATTN OPR HAROLD GARDNER
01CY ATTN LKB KENNETH S.W. CHAMPION
01CY ATTN OPR ALVA T. STAIR
01CY ATTN PHD JURGEN BUCHAU
01CY ATTN PHD JOHN P. MULLEN

AF WEAPONS LABORATORY
KIRTLAND AFT, NM 87117
01CY ATTN SUL
01CY ATTN CA ARTHUR H. GUENTHER
01CY ATTN NTYCE 1LT. G. KRAJEI

AFTAC
PATRICK AFB, FL 32925
01CY ATTN TF/MAJ WILEY
01CY ATTN TN

AIR FORCE AVIONICS LABORATORY
WRIGHT-PATTERSON AFB, OH 45433
01CY ATTN AAD WADE HUNT
01CY ATTN AAD ALLEN JOHNSON

DEPUTY CHIEF OF STAFF
RESEARCH, DEVELOPMENT, & ACQ
DEPARTMENT OF THE AIR FORCE
WASHINGTON, D.C. 20330
01CY ATTN AFRDQ

HEADQUARTERS
ELECTRONIC SYSTEMS DIVISION
DEPARTMENT OF THE AIR FORCE
HANSCOM AFB, MA 01731
01CY ATTN J. DEAS

HEADQUARTERS
ELECTRONIC SYSTEMS DIVISION/YSEA
DEPARTMENT OF THE AIR FORCE
HANSCOM AFB, MA 01732
01CY ATTN YSEA

HEADQUARTERS
ELECTRONIC SYSTEMS DIVISION/DC
DEPARTMENT OF THE AIR FORCE
HANSCOM AFB, MA 01731
01CY ATTN DCKC MAJ J.C. CLARK

COMMANDER
FOREIGN TECHNOLOGY DIVISION, AFSC
WRIGHT-PATTERSON AFB, OH 45433
01CY ATTN NICD LIBRARY
01CY ATTN ETDP B. BALLARD

COMMANDER
ROME AIR DEVELOPMENT CENTER, AFSC
GRIFFISS AFB, NY 13441
01CY ATTN DOC LIBRARY/TSLD
01CY ATTN OCSE V. COYNE

SAMSO/SZ
POST OFFICE BOX 92960
WORLDWAY POSTAL CENTER
LOS ANGELES, CA 90009
(SPACE DEFENSE SYSTEMS)
01CY ATTN SZJ

STRATEGIC AIR COMMAND/XPFS
OFFUTT AFB, NB 68113
01CY ATTN ADWATE MAJ BRUCE BAUER
01CY ATTN NRT
01CY ATTN DOK CHIEF SCIENTIST

SAMSO/SK
P.O. BOX 92960
WORLDWAY POSTAL CENTER
LOS ANGELES, CA 90009
01CY ATTN SKA (SPACE COMM SYSTEMS)
M. CLAVIN

SAMSO/MN
NORTON AFB, CA 92409
(MINUTEMAN)
01CY ATTN MNNL

COMMANDER
ROME AIR DEVELOPMENT CENTER, AFSC
HANSCOM AFB, MA 01731
01CY ATTN EEP A. LORENTZEN

DEPARTMENT OF ENERGY
LIBRARY ROOM G-042
WASHINGTON, D.C. 20545
01CY ATTN DOC CON FOR A. LABOWITZ

DEPARTMENT OF ENERGY
ALBUQUERQUE OPERATIONS OFFICE
P.O. BOX 5400
ALBUQUERQUE, NM 87115
01CY ATTN DOC CON FOR D. SHERWOOD

EG&G, INC.
LOS ALAMOS DIVISION
P.O. BOX 809
LOS ALAMOS, NM 85544
01CY ATTN DOC CON FOR J. BREEDLOVE

UNIVERSITY OF CALIFORNIA
LAWRENCE LIVERMORE LABORATORY
P.O. BOX 808
LIVERMORE, CA 94550
01CY ATTN DOC CON FOR TECH INFO DEPT
01CY ATTN DOC CON FOR L-389 R. OTT
01CY ATTN DOC CON FOR L-31 R. HAGER
01CY ATTN DOC CON FOR L-46 F. SEWARD

LOS ALAMOS NATIONAL LABORATORY
P.O. BOX 1663
LOS ALAMOS, NM 87545
01CY ATTN DOC CON FOR J. WOLCOTT
01CY ATTN DOC CON FOR R.F. TASCHEK
01CY ATTN DOC CON FOR E. JONES
01CY ATTN DOC CON FOR J. MALIK
01CY ATTN DOC CON FOR R. JEFFRIES
01CY ATTN DOC CON FOR J. ZINN
01CY ATTN DOC CON FOR P. KEATON
01CY ATTN DOC CON FOR D. WESTERVELT
01CY ATTN D. SAPPENFIELD

SANDIA LABORATORIES
P.O. BOX 5800
ALBUQUERQUE, NM 87115
01CY ATTN DOC CON FOR W. BROWN
01CY ATTN DOC CON FOR A. THORNBROUGH
01CY ATTN DOC CON FOR T. WRIGHT
01CY ATTN DOC CON FOR D. DAHLGREN
01CY ATTN DOC CON FOR 3141
01CY ATTN DOC CON FOR SPACE PROJECT DIV

SANDIA LABORATORIES
LIVERMORE LABORATORY
P.O. BOX 969
LIVERMORE, CA 94550
01CY ATTN DOC CON FOR B. MURPHEY
01CY ATTN DOC CON FOR T. COOK

OFFICE OF MILITARY APPLICATION
DEPARTMENT OF ENERGY
WASHINGTON, D.C. 20545
01CY ATTN DOC CON DR. YO SONG

OTHER GOVERNMENT

DEPARTMENT OF COMMERCE
NATIONAL BUREAU OF STANDARDS
WASHINGTON, D.C. 20234
01CY (ALL CORRES: ATTN SEC OFFICER FOR)

INSTITUTE FOR TELECOM SCIENCES
NATIONAL TELECOMMUNICATIONS & INFO ADMIN
BOULDER, CO 80303
01CY ATTN A. JEAN (UNCLASS ONLY)
01CY ATTN W. UTLAUT
01CY ATTN D. CROMBIE
01CY ATTN L. BERRY

NATIONAL OCEANIC & ATMOSPHERIC ADMIN
ENVIRONMENTAL RESEARCH LABORATORIES
DEPARTMENT OF COMMERCE
BOULDER, CO 80302
01CY ATTN R. GRUBB
01CY ATTN AERONOMY LAB G. REID

DEPARTMENT OF DEFENSE CONTRACTORS

AEROSPACE CORPORATION
P.O. BOX 92957
LOS ANGELES, CA 90009
01CY ATTN I. GARFUNKEL
01CY ATTN T. SALMI
01CY ATTN V. JOSEPHSON
01CY ATTN S. BOWER
01CY ATTN D. OLSEN

ANALYTICAL SYSTEMS ENGINEERING CORP
5 OLD CONCORD ROAD
BURLINGTON, MA 01803
01CY ATTN RADIO SCIENCES

AUSTIN RESEARCH ASSOC., INC.
1901 RUTLAND DRIVE
AUSTIN, TX 78758
01CY ATTN L. SLOAN
01CY ATTN R. THOMPSON

BERKELEY RESEARCH ASSOCIATES, INC.
P.O. BOX 983
BERKELEY, CA 94701
01CY ATTN J. WORKMAN
01CY ATTN C. PRETTIE
01CY ATTN S. BRECHT

BOEING COMPANY, THE
P.O. BOX 3707
SEATTLE, WA 98124
01CY ATTN G. KEISTER
01CY ATTN D. MURRAY
01CY ATTN G. HALL
01CY ATTN J. KENNEY

CHARLES STARK DRAPER LABORATORY, INC.
555 TECHNOLOGY SQUARE
CAMBRIDGE, MA 02139
01CY ATTN D.B. COX
01CY ATTN J.P. GILMORE

COMSAT LABORATORIES
LINTHICUM ROAD
CLARKSBURG, MD 20734
01CY ATTN G. HYDE

CORNELL UNIVERSITY
DEPARTMENT OF ELECTRICAL ENGINEERING
ITHACA, NY 14850
01CY ATTN D.T. FARLEY, JR.

ELECTROSPACE SYSTEMS, INC.
BOX 1359
RICHARDSON, TX 75080
01CY ATTN H. LOGSTON
01CY ATTN SECURITY (PAUL PHILLIPS)

EOS TECHNOLOGIES, INC.
606 Wilshire Blvd.
Santa Monica, Calif 90401
01CY ATTN C.B. GABBARD

ESL, INC.
495 JAVA DRIVE
SUNNYVALE, CA 94086
01CY ATTN J. ROBERTS
01CY ATTN JAMES MARSHALL

GENERAL ELECTRIC COMPANY
SPACE DIVISION
VALLEY FORGE SPACE CENTER
GODDARD BLVD KING OF PRUSSIA
P.O. BOX 8555
PHILADELPHIA, PA 19101
01CY ATTN M.H. BORTNER SPACE SCI LAB

GENERAL ELECTRIC COMPANY
P.O. BOX 1122
SYRACUSE, NY 13201
01CY ATTN F. REIBERT

GENERAL ELECTRIC TECH SERVICES CO., INC.
HMES
COURT STREET
SYRACUSE, NY 13201
  01CY ATTN G. MILLMAN

GEOPHYSICAL INSTITUTE
UNIVERSITY OF ALASKA
FAIRBANKS, AK 99701
  (ALL CLASS ATTN: SECURITY OFFICER)
  01CY ATTN T.N. DAVIS (UNCLASS ONLY)
  01CY ATTN TECHNICAL LIBRARY
  01CY ATTN NEAL BROWN (UNCLASS ONLY)

GTE SYLVANIA, INC.
ELECTRONICS SYSTEMS GRP-EASTERN DIV
77 A STREET
NEEDHAM, MA 02194
  01CY ATTN DICK STEINHOF

HSS, INC.
2 ALFRED CIRCLE
BEDFORD, MA 01730
  01CY ATTN DONALD HANSEN

ILLINOIS, UNIVERSITY OF
107 COBLE HALL
150 DAVENPORT HOUSE
CHAMPAIGN, IL 61820
  (ALL CORRES ATTN DAN MCCLELLAND)
  01CY ATTN K. YEH

INSTITUTE FOR DEFENSE ANALYSES
1801 NO. BEAUREGARD STREET
ALEXANDRIA, VA 22311
  01CY ATTN J.M. AEIN
  01CY ATTN ERNEST BAUER
  01CY ATTN HANS WOLFARD
  01CY ATTN JOEL BENGSTON

INTL TEL & TELEGRAPH CORPORATION
500 WASHINGTON AVENUE
NUTLEY, NJ 07110
  01CY ATTN TECHNICAL LIBRARY

JAYCOR
11011 TORREYANA ROAD
P.O. BOX 85154
SAN DIEGO, CA 92138
  01CY ATTN J.L. SPERLING

JOHNS HOPKINS UNIVERSITY
APPLIED PHYSICS LABORATORY
JOHNS HOPKINS ROAD
LAUREL, MD 20810
  01CY ATTN DOCUMENT LIBRARIAN
  01CY ATTN THOMAS POTEMRA
  01CY ATTN JOHN DASSOULAS

KAMAN SCIENCES CORP
P.O. BOX 7463
COLORADO SPRINGS, CO 80933
  01CY ATTN T. MEAGHER

KAMAN TEMPO-CENTER FOR ADVANCED STUDIES
816 STATE STREET (P.O DRAWER QQ)
SANTA BARBARA, CA 93102
  01CY ATTN DASIAC
  01CY ATTN WARREN S. KNAPP
  01CY ATTN WILLIAM MCNAMARA
  01CY ATTN B. GAMBILL

LINKABIT CORP
10453 ROSELLE
SAN DIEGO, CA 92121
  01CY ATTN IRWIN JACOBS

LOCKHEED MISSILES & SPACE CO., INC
P.O. BOX 504
SUNNYVALE, CA 94088
  01CY ATTN DEPT 60-12
  01CY ATTN D.R. CHURCHILL

LOCKHEED MISSILES & SPACE CO., INC.
3251 HANOVER STREET
PALO ALTO, CA 94304
  01CY ATTN MARTIN WALT DEPT 52-12
  01CY ATTN W.L. IMHOF DEPT 52-12
  01CY ATTN RICHARD G. JOHNSON DEPT 52-12
  01CY ATTN J.B. CLADIS DEPT 52-12

MARTIN MARIETTA CORP
ORLANDO DIVISION
P.O. BOX 5837
ORLANDO, FL 32805
  01CY ATTN R. HEFFNER

M.I.T. LINCOLN LABORATORY
P.O. BOX 73
LEXINGTON, MA 02173
  01CY ATTN DAVID M. TOWLE
  01CY ATTN L. LOUGHLIN
  01CY ATTN D. CLARK

MCDONNEL DOUGLAS CORPORATION
5301 BOLSA AVENUE
HUNTINGTON BEACH, CA 92647
01CY ATTN N. HARRIS
01CY ATTN J. MOULE
01CY ATTN GEORGE MROZ
01CY ATTN W. OLSON
01CY ATTN R.W. HALPRIN
01CY ATTN TECHNICAL LIBRARY SERVICES

MISSION RESEARCH CORPORATION
735 STATE STREET
SANTA BARBARA, CA 93101
01CY ATTN P. FISCHER
01CY ATTN W.F. CREVIER
01CY ATTN STEVEN L. GUTSCHE
01CY ATTN R. BOGUSCH
01CY ATTN R. HENDRICK
01CY ATTN RALPH KILB
01CY ATTN DAVE SOWLE
01CY ATTN F. FAJEN
01CY ATTN M. SCHEIBE
01CY ATTN CONRAD L. LONGMIRE
01CY ATTN B. WHITE

MISSION RESEARCH CORP.
1720 RANDOLPH ROAD, S.E.
ALBUQUERQUE, NEW MEXICO 87106
01CY R. STELLINGWERF
01CY M. ALME
01CY L. WRIGHT

MITRE CORPORATION, THE
P.O. BOX 208
BEDFORD, MA 01730
01CY ATTN JOHN MORGANSTERN
01CY ATTN G. HARDING
01CY ATTN C.E. CALLAHAN

MITRE CORP
WESTGATE RESEARCH PARK
1820 DOLLY MADISON BLVD
MCLEAN, VA 22101
01CY ATTN W. HALL
01CY ATTN W. FOSTER

PACIFIC-SIERRA RESEARCH CORP
12340 SANTA MONICA BLVD.
LOS ANGELES, CA 90025
01CY ATTN E.C. FIELD, JR.

PENNSYLVANIA STATE UNIVERSITY
IONOSPHERE RESEARCH LAB
318 ELECTRICAL ENGINEERING EAST
UNIVERSITY PARK, PA 16802
(NO CLASS TO THIS ADDRESS)
01CY ATTN IONOSPHERIC RESEARCH LAB

PHOTOMETRICS, INC.
4 ARROW DRIVE
WOBURN, MA 01801
01CY ATTN IRVING L. KOFSKY

PHYSICAL DYNAMICS, INC.
P.O. BOX 3027
BELLEVUE, WA 98009
01CY ATTN E.J. FREMOUW

PHYSICAL DYNAMICS, INC.
P.O. BOX 10367
OAKLAND, CA 94610
ATTN A. THOMSON

R & D ASSOCIATES
P.O. BOX 9695
MARINA DEL REY, CA 90291
01CY ATTN FORREST GILMORE
01CY ATTN WILLIAM B. WRIGHT, JR.
01CY ATTN ROBERT F. LELEVIER
01CY ATTN WILLIAM J. KARZAS
01CY ATTN H. ORY
01CY ATTN C. MACDONALD
01CY ATTN R. TURCO
01CY ATTN L. DeRAND
01CY ATTN W. TSAI

RAND CORPORATION, THE
1700 MAIN STREET
SANTA MONICA, CA 90406
01CY ATTN CULLEN CRAIN
01CY ATTN ED BEDROZIAN

RAYTHEON CO.
528 BOSTON POST ROAD
SUDBURY, MA 01776
01CY ATTN BARBARA ADAMS

RIVERSIDE RESEARCH INSTITUTE
330 WEST 42nd STREET
NEW YORK, NY 10036
01CY ATTN VINCE TRAPANI

SCIENCE APPLICATIONS, INC.
1150 PROSPECT PLAZA
LA JOLLA, CA 92037
01CY ATTN LEWIS M. LINSON
01CY ATTN DANIEL A. HAMLIN
01CY ATTN E. FRIEMAN
01CY ATTN E.A. STRAKER
01CY ATTN CURTIS A. SMITH
01CY ATTN JACK MCDOUGALL

SCIENCE APPLICATIONS, INC
1710 GOODRIDGE DR.
MCLEAN, VA 22102
ATTN: J. COCKAYNE

SRI INTERNATIONAL
333 RAVENSWOOD AVENUE
MENLO PARK, CA 94025
01CY ATTN DONALD NEILSON
01CY ATTN ALAN BURNS
01CY ATTN G. SMITH
01CY ATTN R. TSUNODA
01CY ATTN DAVID A. JOHNSON
01CY ATTN WALTER G. CHESNUT
01CY ATTN CHARLES L. RINO
01CY ATTN WALTER JAYE
01CY ATTN J. VICKREY
01CY ATTN RAY L. LEADABRAND
01CY ATTN G. CARPENTER
01CY ATTN G. PRICE
01CY ATTN R. LIVINGSTON
01CY ATTN V. GONZALES
01CY ATTN D. MCDANIEL

TECHNOLOGY INTERNATIONAL CORP
75 WIGGINS AVENUE
BEDFORD, MA 01730
01CY ATTN W.P. BOQUIST

TOYON RESEARCH CO.
P.O. Box 6890
SANTA BARBARA, CA 93111
01CY ATTN JOHN ISE, JR.
01CY ATTN JOEL GARBARINO

TRW DEFENSE & SPACE SYS GROUP
ONE SPACE PARK
REDONDO BEACH, CA 90278
01CY ATTN R. K. PLEBUCH
01CY ATTN S. ALTSCHULER
01CY ATTN D. DEE
01CY ATTN D/ STOCKWELL
SNTF/1575

VISIDYNE
SOUTH BEDFORD STREET
BURLINGTON, MASS 01803
01CY ATTN W. REIDY
01CY ATTN J. CARPENTER
01CY ATTN C. HUMPHREY

END

FILMED

9-84

DTIC